Z. Phys. C 61, 567–577 (1994)

ZEITSCHRIFT
FÜR PHYSIK C

Invariant mass dependence of particle correlations in $\pi^+ p$ and $K^+ p$ interactions at 250 GeV/c

EHS/NA22 Collaboration

I.V. Ajinenko[5], F. Botterweck[4,a], M. Charlet[4,b], P.V. Chliapnikov[5], E.A. De Wolf[1,c], K. Dziunikowska[2,d], A.M.F. Endler[6], Z.G. Garutchava[7], G.R. Gulkanyan[8], J.K. Karamyan[8], D. Kisielewska[2,d], W. Kittel[4], F.K. Rizatdinova[3], E.K. Shabalina[3], L.N. Smirnova[3], A. Tomaradze[7,e], F. Verbeure[1]

[1] Department of Physics, Universitaire Instelling Antwerpen, B-2610 Wilrijk and Inter-University Institute for High Energies, B-1050 Brussels, Belgium
[2] Institute of Physics and Nuclear Technique of Academy of Mining and Metallurgy and Institute of Nuclear Physics, PL-30055 Krakow, Poland
[3] Nucl. Phys. Institute, Moscow State University, 119899 Moscow, Russia
[4] University of Nijmegen and NIKHEF-H, NL-6525 ED Nijmegen, The Netherlands
[5] Institute for High Energy Physics, 142284 Protvino, Russia
[6] Centro Brasileiro de Pesquisas Fisicas, 22290 Rio de Janeiro, Brazil
[7] Institute of High Energy Physics of Tbilisi State University, 380086 Tbilisi, Georgia
[8] Institute of Physics, 375036 Yerevan, Armenia

Received 11 October 1993

Abstract. We study two- and three-particle correlations as a function of invariant mass. Using data on $\pi^+ p$ and $K^+ p$ collisions at 250 GeV/c, we compare correlation functions and normalised factorial cumulants for various charge combinations. Strong positive correlations are observed only at small invariant masses. The normalised cumulants for "exotic" $[(--), (++)]$ and "non-exotic" pairs $(+-)$ and triplets decrease in power-like fashion with increasing invariant mass. The mass dependence is not incompatible with the power-law behaviour as expected in a Dual Mueller-Regge framework. Comparison with FRITIOF reveals strong disagreements, which are due to too large production rates of resonances, such as ρ^0 and η, and the absence of a Bose-Einstein low-mass enhancement in JETSET.

1 Introduction

For many years, correlations among hadrons produced in high-energy multi-particle processes have been studied in a variety of variables. Of obvious importance are analyses of multiparticle spectra in terms of the invariant mass of two- and more particle systems, which allowed identification of hadronic resonances.

Studies of correlations in rapidity have helped to establish the fruitful concept of short-range order in momentum space, a dynamical property already present in the earliest multiperipheral pictures of particle production, later extended to ladder diagrams with Regge exchanges. In these, propagators are functions of nearest-neighbour invariant-masses which, at high energy and large mass, are conveniently expressed in terms of rapidity distances.

Correlations attributed to Bose-Einstein symmetrisation of identical boson amplitudes have been much discussed in the literature (for recent reviews see [1, 2]). They are often studied in terms of the difference of particle-pair four-momenta, a traditional choice being $Q_{ij}^2 = -(q_i - q_j)^2$.

Recently, correlation studies have attracted renewed attention in connection with the search for self-similar particle-density fluctuation phenomena, commonly known as "Intermittency" [3, 4]. Intermittency means that the normalised factorial moments F_q of the multiplicity distribution in a phase-space volume δ are power-behaved

$$F_q(\delta) \propto \delta^{-\phi_q}, \quad (\phi_q > 0) \tag{1}$$

over a range of scales, down to the experimental resolution. This further implies that the q-particle densities and correlation functions are singular in the limit $\delta \to 0$. The present status of this field is reviewed in [5].

A significant step towards better understanding of the physics behind intermittency was made by Fiałkowski [6]. Using data in three-dimensional phase space on μp, π/Kp, pA and AA collisions, he noted that F_2 shows a

---

[a] Now at Universitaire Instelling Antwerpen
[b] EC Guest Scientist
[c] Onderzoeksleider NFWO, Belgium
[d] Partially supported by grants from CPBP 01.06 anf 01.09
[e] Also at Universitaire Instelling Antwerpen

surprisingly high degree of "universality". Writing $F_2(\delta)$ as

$$F_2(\delta)=A+B\delta^{-\phi_2}, \tag{2}$$

ϕ_2 was found to be around 0.4–0.5 in all processes considered. The B-values also turn out to be quite similar. The author, therefore, speculated that intermittency may be a "universal collective" effect.

As remarked in [6], δ in (2) is related, albeit non-uniquely, to Q^2 or $M=\sqrt{Q^2+4\mu^2}$, the invariant mass of the particle pairs (μ is the pion mass). The functional form of (2) would then mean that the normalised two-particle cumulant K_2 is power-behaved in M or in Q^2. The latter is singular at $Q^2=0$, while the former remains finite at threshold. This argument suggests that it may be rewarding to study correlation functions and factorial moments directly in terms of invariant mass. This is the subject of the present paper.

The idea to study correlations as a function of invariant-mass was, to our knowledge, first used in [7]. This analysis was based on low statistics pp data at 205 GeV/c. It demonstrated that the factorial cumulant $K_2\equiv F_2-1$ (see further below) follows an approximate power law with very different powers for like-charge ("exotic") and unlike-charge ("non-exotic") hadron pairs. In [7] this is written as:

$$K_2(M)\propto(M^2)^{\alpha_X(0)-1}. \tag{3}$$

The notation reminds of the interpretation of (3) in terms of the Mueller-Regge formalism. The power $\alpha_X(0)$ is the appropriate Regge-intercept; $X=R$ for non-exotic pairs and $X=E$ for exotic ones. The ratio K_2^{--}/K_2^{+-} was further seen to fall as M^{-2}, consistent with $\alpha_R(0)-\alpha_E(0)=1$. Not relying on Mueller-Regge theory, the authors argued that most of the correlations at small M are due to resonance decays into three or more pions and to interference of amplitudes [8].

In this paper we study the invariant-mass dependence of two- and three-particle correlations in a combined sample of π^+p and K^+p interactions at $\sqrt{s}=22$ GeV. The experimental procedure and the formalism used are described in Sect. 2. Results and their implications for intermittency are discussed in Sect. 3. The data are compared to the Lund FRITIOF model for hadron-hadron interactions in Sect. 4. Conclusions and a summary are given in Sect. 5.

2 Experimental procedure

2.1 Event selection

In this CERN experiment, the European Hybrid Spectrometer (EHS) is equipped with the Rapid Cycling Bubble Chamber (RCBC) as an active vertex detector and exposed to a 250 GeV/c tagged positive, meson enriched beam. In data taking, a minimum bias interaction trigger is used. The details of the spectrometer and the trigger can be found in previous publications [9, 10].

Charged particle tracks are reconstructed from hits in the wire- and drift-chambers of the two lever-arm magnetic spectrometer and from measurements in the bubble chamber. The average momentum resolution $\langle\Delta p/p\rangle$ varies from a maximum of 2.5% at 30 GeV/c to around 1.5% above 100 GeV/c.

Events are accepted for the analysis when measured and reconstructed charge multiplicity are the same, charge balance is satisfied, no electron is detected among the secondary tracks and the number of reconstructed tracks rejected by our quality criteria is at most 0, 1, 1, 2 and 3 for events with charge multiplicity 2, 4, 6, 8 and >8, respectively. Losses of events during measurement and reconstruction are corrected for using the topological cross sections [9]. Elastic events are excluded. Furthermore, an event is called single-diffractive, and excluded from the sample, if the total charge multiplicity is smaller than 8 and at least one of the positive tracks has $|x_F|>0.88$. After these cuts, we remain with a sample of inelastic non-single-diffractive π^+/K^+p interactions consisting of 114 472 events. The results presented below pertain to the combined π^+p and K^+p samples.

For momenta $p_{\mathrm{LAB}}<0.7$ GeV/c, the range in the bubble chamber and/or the change of track curvature is used for proton identification. In addition, a visual ionization scan has been used for $p_{\mathrm{LAB}}<1.2$ GeV/c on the full K^+p and 62% of the π^+p sample. Positive particles with $p_{\mathrm{LAB}}>150$ GeV/c are given the identity of the beam particle. Other particles with momenta $p_{\mathrm{LAB}}>1.2$ GeV/c are not identified in the present analysis and are treated as pions. Identified protons are removed from the track sample.

2.2 The correlation function in invariant mass

The two-particle correlation function for hadrons a and b (assumed to be pions in the following) is defined as the inclusive coincidence rate per collision, minus the rate expected for uncorrelated hadrons a and b:

$$C_2^{ab}(q_1,q_2)\equiv\rho_2^{ab}(q_1,q_2)-\rho_1^a(q_1)\,\rho_1^b(q_2). \tag{4}$$

In this expression $q_i(p_i,E_i)$, $(i=1,2)$, are the four-momenta of the two hadrons. The invariant two-particle inclusive density is

$$\rho_2^{ab}(q_1,q_2)=\frac{E_1E_2}{\sigma_I}\,\frac{\mathrm{d}\sigma}{\mathrm{d}^3p_1\,\mathrm{d}^3p_2}. \tag{5}$$

The invariant single-particle inclusive density is

$$\rho_1^{a,b}(q)=\frac{E}{\sigma_I}\,\frac{\mathrm{d}^3\sigma}{\mathrm{d}^3p}, \tag{6}$$

with σ_I the inelastic cross section. The densities (5–6) are normalised as follows

$$\iint\rho_2(q_1,q_2)\,\frac{\mathrm{d}^3p_1}{E_1}\,\frac{\mathrm{d}^3p_2}{E_2}=\langle n_a(n_b-\delta_{ab})\rangle, \tag{7}$$

$$\int\rho_1^{a,b}(q)\,\frac{\mathrm{d}^3p}{E}=-\langle n_{a,b}\rangle, \tag{8}$$

with $\delta_{ab}=1$ if particles a and b are of the same type, and $\delta_{ab}=0$ otherwise. The integrations and the averages are taken over full or part of phase space.

The function C_2 in (4) depends on six dependent variables, a common choice being the c.m. energy, $\sqrt{s}$, the c.m. rapidities y_1 and y_2, the magnitudes p_{T_1}, p_{T_2}, the transverse momenta, and their relative azimuthal angle, Φ.

Most often, measurements of C_2 average over the transverse degrees of freedom, leaving only the longitudinal momentum (p_L) or rapidity dependence. The resulting correlation function is

$$C_2^{ab}(y_1, y_2)=\int \mathrm{d}^2 p_{T_1} \int \mathrm{d}^2 p_{T_2}\, C_2^{ab}(q_1, q_2)\,. \tag{9}$$

It is important to note that any structure which occurs at fixed invariant mass M ($M^2=(q_1+q_2)^2$), due e.g. to resonances or resonance reflections, is in general smeared out in the integrated correlation function (9). In fact, $C_2(y_1, y_2)$ depends mainly on the angular decay of the system and much less so on the mass spectrum. For isotropic decay it has the familiar approximately Gaussian shape.

Here, we are interested in correlation effects in invariant mass near threshold and shall, therefore, keep M (or Q^2, see below) in the set of independent variables describing C_2. We further keep p_{T_1}, p_{T_2} and Φ in the set and average over the longitudinal momentum of the system with mass M. The relation between M and $\Delta y=y_1-y_2$ is

$$M^2=2\mu^2-2\,p_{T_1}p_{T_2}\cos\Phi+2\,m_{T_1}m_{T_2}\cosh\Delta y\,, \tag{10}$$

with $m_T^2=\mu^2+p_T^2$. For large M and large Δy, one has

$$M^2\sim\exp(|\Delta y|)\,. \tag{11}$$

However, for small M or small Δy, relevant in intermittency studies, the relation between these variables is greatly influenced by the values of the transverse momenta. From (10) one also sees that selection of particles with small transverse momentum will introduce a shift towards small values in the invariant mass distribution integrated over Φ.

When (4) is integrated over the p_{T_1}, p_{T_2} and Φ, and over the longitudinal momentum of the pair, C_2 becomes a function only of M, at fixed $\sqrt{s}$:

$$C_2^{ab}(M)=\rho_2^{ab}(M)-\rho_1^a\otimes\rho_1^b(M)\,. \tag{12}$$

In (12), ρ_2^{ab} is the familiar normalised two-particle invariant-mass spectrum. The second term describes the uncorrelated "background" and is at fixed mass of the pair given by:

$$\rho_1^a\otimes\rho_1^b(M)=\int\frac{\mathrm{d}^3p_1}{E_1}\int\frac{\mathrm{d}^3p_2}{E_2}\,\rho_1^a(q_1)\,\rho_1^b(q_2)\times\delta\{[(q_1+q_2)^2]^{1/2}-M\}\,, \tag{13}$$

with the normalisation:

$$\int\rho_1^a\otimes\rho_1^b\,dM=\langle n_a\rangle\langle n_b\rangle\,. \tag{14}$$

The integral over M of $C_2(M)$ in (12) is equal to the second-order integrated factorial cumulant or Mueller moment [11],

$$C_2^{ab}=\int C_2^{ab}(M)\,dM=\langle n_a(n_b-\delta_{ab})\rangle-\langle n_a\rangle\langle n_b\rangle\,. \tag{15}$$

In direct correspondence with normalised factorial moments and cumulants in intermittency analyses, we consider below the normalised functions

$$K_2^{ab}(M)=F_2^{ab}(M)-1\,, \tag{16}$$

with

$$F_2^{ab}(M)=\rho_2^{ab}(M)/\rho_1^a\otimes\rho_1^b(M)\,. \tag{17}$$

For three-particle systems, we define the "connected" correlation function (or factorial cumulant) in the usual way

$$\begin{aligned}C_3^{abc}(q_1,q_2,q_3)\equiv\rho_3^{abc}&-\rho_1^a(q_1)\,\rho_2^{bc}(q_2,q_3)\\&-\rho_1^b(q_2)\,\rho_2^{ca}(q_1,q_3)\\&-\rho_1^c(q_3)\,\rho_2^{ab}(q_1,q_2)\\&+2\,\rho_1^a(q_1)\,\rho_1^b(q_2)\,\rho_1^c(q_3)\,.\end{aligned} \tag{18}$$

Integration over all variables, except $M^2=(q_1+q_2+q_3)^2$ yields

$$C_3(M)\equiv\rho_3(M)-\{\rho_1^a\otimes\rho_2^{bc}(M)+\text{perm.}\}+2\,\rho_1^a\otimes\rho_1^b\otimes\rho_1^c(M)\,, \tag{19}$$

$$K_3(M)=C_3(M)/\rho_1^a\otimes\rho_1^b\otimes\rho_1^c(M)\,. \tag{20}$$

To calculate the background term (13) one may apply a Monte-Carlo method as in [7]. Here we use a "track-pool" or "event-mixing" technique, similar to that used in studes of Bose-Einstein (BE) correlations and in the "correlation-integral" method [12]. The procedure is as follows. A pool of particle four-vectors is constructed from a large number of events. Then, to build an "uncorrelated" event, track-multiplicities N_i for particles of type i are chosen according to a Poissonian with a fixed average, and N_i particles of the desired type are randomly selected with equal probability from the "pool", ensuring that each particle originates from a different event. The fake events then undergo the same treatment as the real events. The mass-spectra $\rho_2(M)$ and $\rho_1\otimes\rho_1(M)$ are normalised to their respective experimental values (7) and (14) in the studied kinemtatical region.

The same technique is easily generalised to three- or higher-order correlation functions. For example, a term $\rho_1^a\otimes\rho_2^{bc}(M)$ in (19) is calculated taking from each event one track of type (b) and type (c), and a third track of type (a) from another event.

Before describing the data, it is useful to elaborate somewhat on the physical meaning of (12) [7, 8]. For independently produced particles $C_2(M)$ is necessarily zero if kinematical constraints can be neglected. If par-

ticles are produced exclusively via the two-body decay of a resonance or cluster (hardly realistic for $\pi^{\pm}\pi^{\pm}$-pairs), then $C_2(M)$ measures directly the dynamical correlation within the cluster. Two particles originating from different resonances contribute only to the background (provided one may neglect interference effects). Not eliminated from C_2 are, therefore, those pairs which are the decay products of an m-particle resonance ($m \geqq 3$). The function C_3 has an analogous meaning.

3 Experimental results

3.1 Invariant-mass dependence of C_2

To illustrate the method and the general trend of the data, we show in Fig. 1 $\rho_2(M)$, $\rho_1 \otimes \rho_1(M)$ and $C_2(M)$ for $(--)$ and $(+-)$ charge-combinations in full phase space. The distributions $\rho_2(M)$ and $\rho_1 \otimes \rho_1(M)$ evidently extend to large M-values, but we shall be mainly interested in the region below 1 GeV.

One notices that $\rho_2(M)$ and $\rho_1 \otimes \rho_1(M)$ become equal, within errors, above a relatively small value of M. This gives confidence in the usefulness of the function $C_2(M)$ as a measure of dynamical correlation effects.

The function $C_2^{--}(M)$ is largest at threshold, slightly negative near $M \sim 0.8$ GeV and zero for $M > 1.5$ GeV; $\rho_2^{+-}(M)$, and $C_2^{+-}(M)$ in particular, reveal a clear ρ^0 signal. These functions are nearly zero for $M \geqq 1.5$ GeV.

Figure 2 compares in more detail C_2 for various charge combinations. Here, and for all following results, we limit the single particle c.m. rapidity to $|y| < 2$, unless specified otherwise. One observes that $C_2^{++}(M)$ and $C_2^{--}(M)$ practically coincide. In contrast, $C_2^{+-}(M)$ drops to zero at threshold; otherwise it is much larger, and has a very different shape compared to $C_2^{\pm\pm}$. Qualitatively, this is easily understood. Besides direct contributions from resonances in the $(+-)$-channel, additional correlations are generated by other states (such as η, η', ω, A_2,...) decaying into higher multiplicity channels. An anologous contribution, but much smaller in magnitude and concentrated at lower mass is expected for like-sign pairs. For these, in addition, interference effects due to Bose-Einstein symmetrisation of resonance- and prompt-particle production amplitudes will enhance the invariant-mass region close to threshold [8, 13].

For the second-order Mueller moment we obtain $C_2^{--} = 0.79 \pm 0.05\,(0.71 \pm 0.04)$, $C_2^{++} = 0.89 \pm 0.08\,(0.74 \pm 0.02)$, $C_2^{+-} = 3.65 \pm 0.07\,(2.68 \pm 0.05)$ for all M (for $M < 0.8$ GeV). Consequently, the region below 0.8 GeV in $C_2^{--}(M)$ or $C_2^{++}(M)$ accounts for $\sim 90\%$ of all correlations; for $C_2^{+-}(M)$ this is significantly smaller ($\sim 73\%$).

The behaviour of $C_2^{cc}(M)$ in Fig. 2 combines the features of the charge-separated states and is therefore less instructive*. Nevertheless, in many intermittency analyses charges are not distinguished. We shall, therefore, continue to present (cc)-data in the rest of the paper.

It is instructive to compare the results presented in Fig. 2 with our previous study of C_2 in rapidity space. In

* Note that $C_2^{cc} \equiv C_2^{++} + C_2^{--} + 2\,C_2^{+-}$

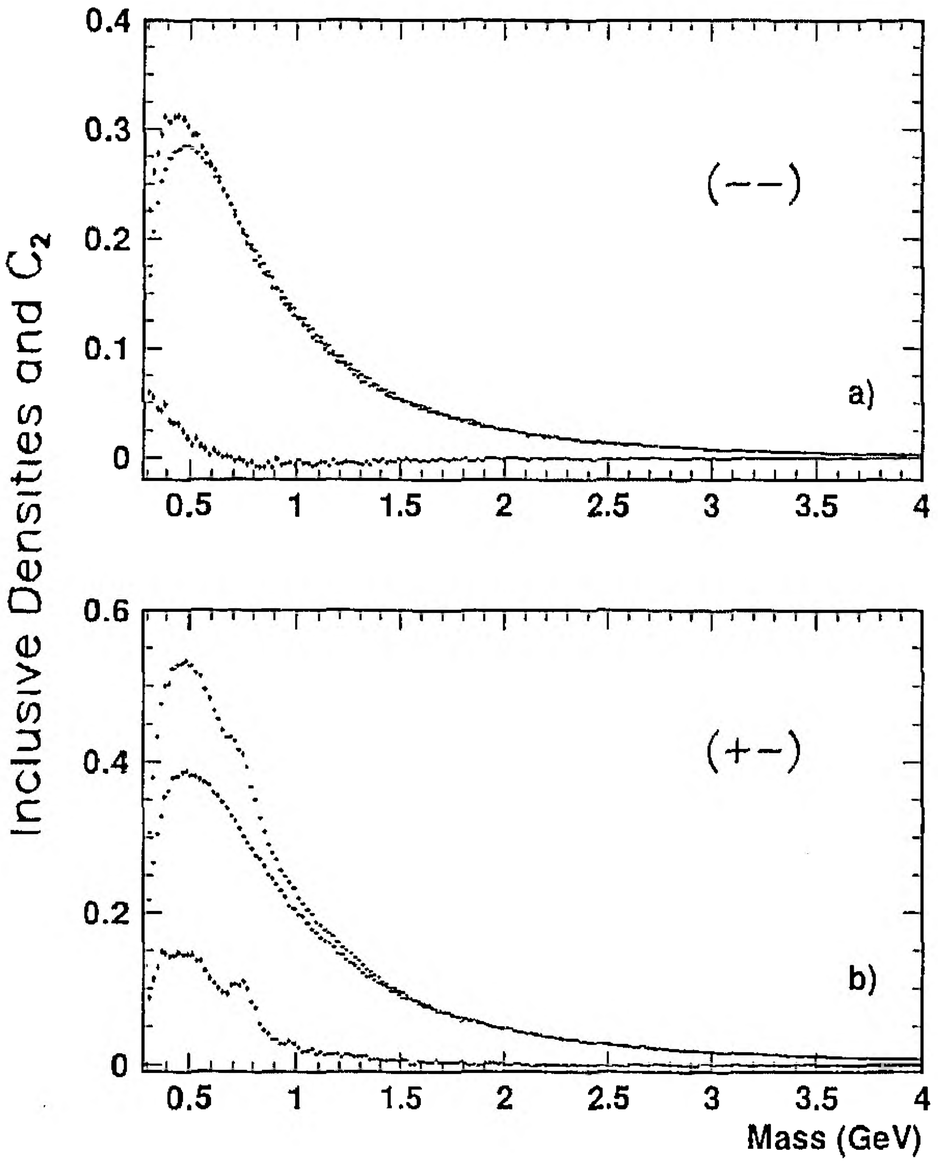

Fig. 1a, b. The densities $\rho_2(M)$ (upper), $\rho_1 \otimes \rho_1(M)$ (middle) and the correlation function $C_2(M)$ (lower) for $(--)$- and $(+-)$-pairs produced in $\pi^+ p$ and $K^+ p$ interactions (combined) in full phase space

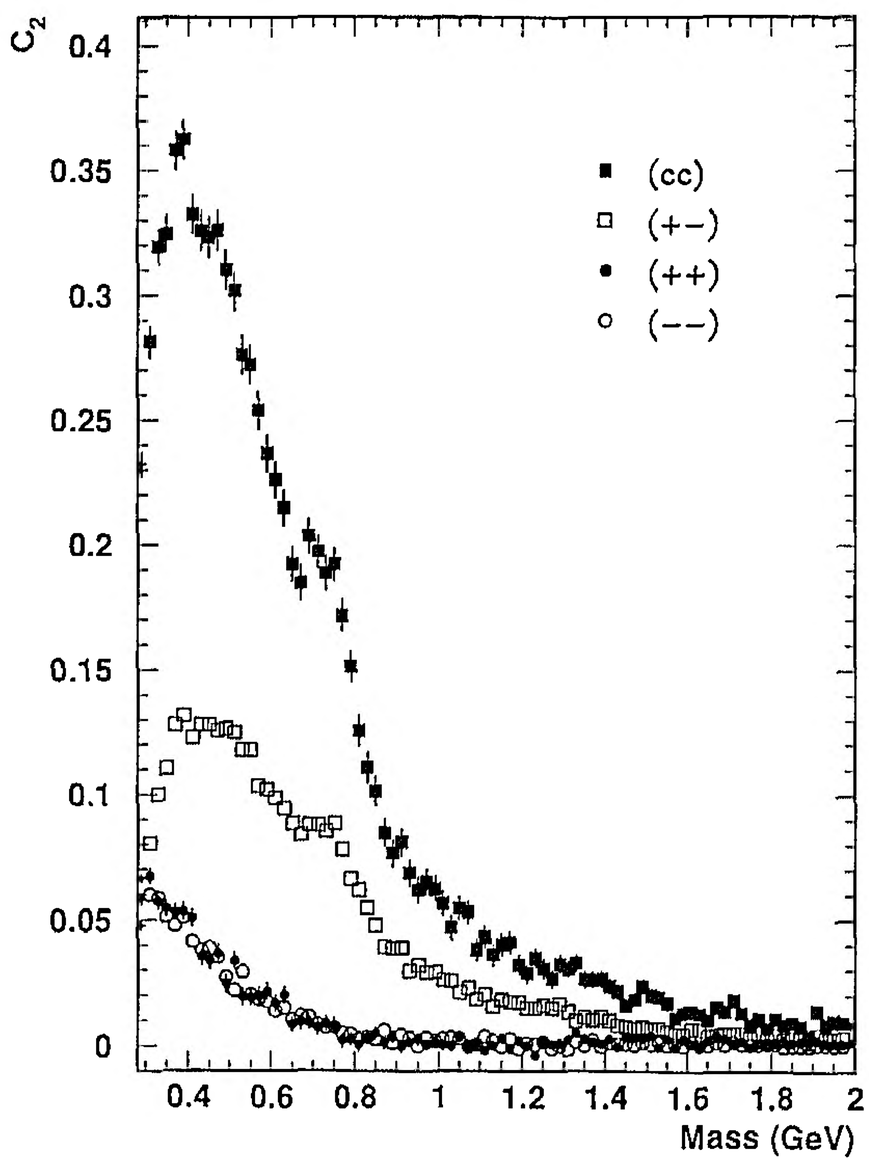

Fig. 2. The correlation function $C_2(M)$ for the indicated charge combinations for particles with c.m. rapidity $|y_i| < 2$ $(i = 1, 2)$

[14] we found that the correlation functions $C_2(y_1, y_2)$ for different charge-states, while differing in absolute values near $y_1 = 0$, all have a similar Gaussian shape with a dispersion ranging from ~ 0.8 for $(--)$-pairs to ~ 1 for $(+-)$-pairs. Figure 2 illustrates that the similarity in rapidity space is superficial and hides the true nature of the dynamical correlations. The correlation functions for like- and unlike-sign pairs indeed differ strongly when studied in terms of invariant mass, for the reasons mentioned earlier in this section.

3.2 Normalised second-order factorial cumulants

Intermittency studies deal with normalised factorial moments and factorial cumulants in small domains of phase space. We, therefore, turn to a presentation of the data on the normalised cumulant function $K_2(M)$.

Figure 3 shows $K_2^{+-}(M)$, $K_2^{cc}(M)$, $K_2^{--}(M)$ and $K_2^{++}(M)$ for particles with rapidity $|y| < 2$ (open symbols) and $|y| < 0.5$ (solid symbols). These figures demonstrate that also $K_2(M)$ is very different for like- and unlike-charge pairs.

For like-charge pairs, K_2 drops in a power-like manner and is close to zero for masses around 1 GeV. Unlike-charge pairs show a clear ρ^0 contribution in particular for $|y| < 0.5$. Otherwise, the correlation function has a much weaker M-dependence than like-charge pairs. For all charge combinations, the correlation is stronger for $|y| < 0.5$ than for $|y| < 2$.

The lines in Fig. 3 are fits by a power-law

$$K_2(M) = A(1/M^2)^{\beta}. \tag{21}$$

The best-fit parameters are collected in the first four lines of Table 1. Lines 5 and 12 (see further) are results of a fit using invariant-mass bins of 4 MeV.

Figure 4, where the ratio $K_2^{--}(M)/K_2^{+-}(M)$ is plotted (for $|y| < 2$) offers a further illustration of the different M-dependence of the like- and unlike-charge correlation function. The curve represents the function (21)

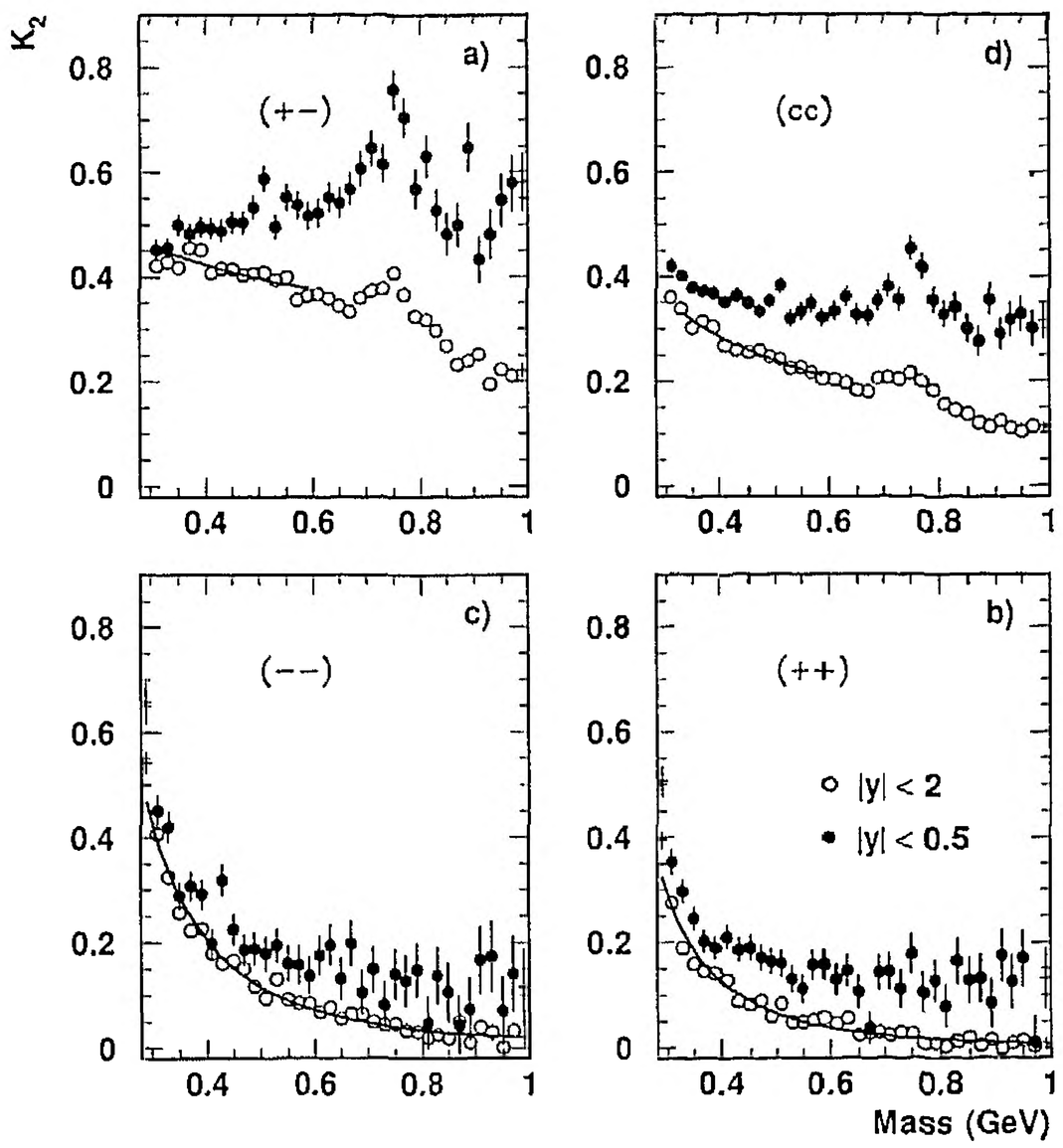

Fig. 3a–d. The normalised second-order factorial cumulant versus invariant mass for particles with c.m. rapidity $|y_i| < 2$ and $|y_i| < 0.5$, respectively. Lines are fits by $A(1/M^2)^{\beta}$ (see Table 1)

with $\beta = 1.02 \pm 0.06$, fitted in the range $0.32 < M < 0.8$ GeV. The value of β is consistent with unity, a value often quoted for the difference in Regge-intercept of an "exotic" and "standard" (ρ, f) trajectory [7]. We shall not further elaborate on a possible Mueller-Regge interpreation (see [7]) which is considered to be doubtful at small M, but merely note that i) the Dual Mueller-Regge approach, with factorisation, leads in a natural way to power-law dependence in invariant mass of the correlation functions, ii) the data in [7], and those presented here, are not in contradiction with this picture.

Table 1. Fits with the form $A(1/M^2)^{\beta}$ to the second- and third-order factorial cumulant $K_2(M)$ and $K_3(M)$ in M^+p interactions at 250 GeV/c incident beam momentum, in indicated invariant-mass intervals and for various cuts (p_T in GeV/c).

K_2, K_3	M (GeV)	Cut	A	β	χ^2/NDF
cc	0.30–0.6	–	0.136 ± 0.004	0.41 ± 0.02	20/13
$+-$	0.30–0.6	–	0.315 ± 0.010	0.17 ± 0.02	30/11
$++$	0.34–1.0	–	0.011 ± 0.001	1.30 ± 0.07	25/31
$--$	0.34–1.0	–	0.024 ± 0.001	1.15 ± 0.05	32/31
$--$	0.28–1.0	–	0.019 ± 0.002	1.29 ± 0.04	226/178
$--$	0.28–0.6	$\Phi < 45°$	0.014 ± 0.001	2.45 ± 0.24	60/34
$--$	0.28–1.0	$45° < \Phi < 135°$	0.022 ± 0.002	1.32 ± 0.05	42/34
$+-$	0.34–1.0	$\Phi < 45°$	0.080 ± 0.006	0.72 ± 0.05	23/15
$+-$	0.34–1.0	$45° < \Phi < 135°$	0.26 ± 0.01	0.35 ± 0.02	31/15
$--$	0.28–1.0	$p_T < 0.15$	0.013 ± 0.001	1.54 ± 0.24	41/34
$--$	0.28–1.0	$0.15 < p_T < 0.3$	0.022 ± 0.004	1.36 ± 0.08	43/34
$--$	0.28–1.0	$p_T > 0.15$	0.015 ± 0.002	1.35 ± 0.07	202/178
$---$	0.42–1.0	–	0.005 ± 0.002	3.37 ± 0.32	41/26
$+++$	0.42–1.0	–	0.015 ± 0.007	3.84 ± 0.99	28/26
$++-$	0.42–1.0	–	0.085 ± 0.004	1.16 ± 0.06	10/26
$--+$	0.42–0.8	–	0.12 ± 0.02	1.0 ± 0.1	11/15
$\frac{--}{+-}$	0.32–0.8	–	0.07 ± 0.01	1.02 ± 0.06	25/22

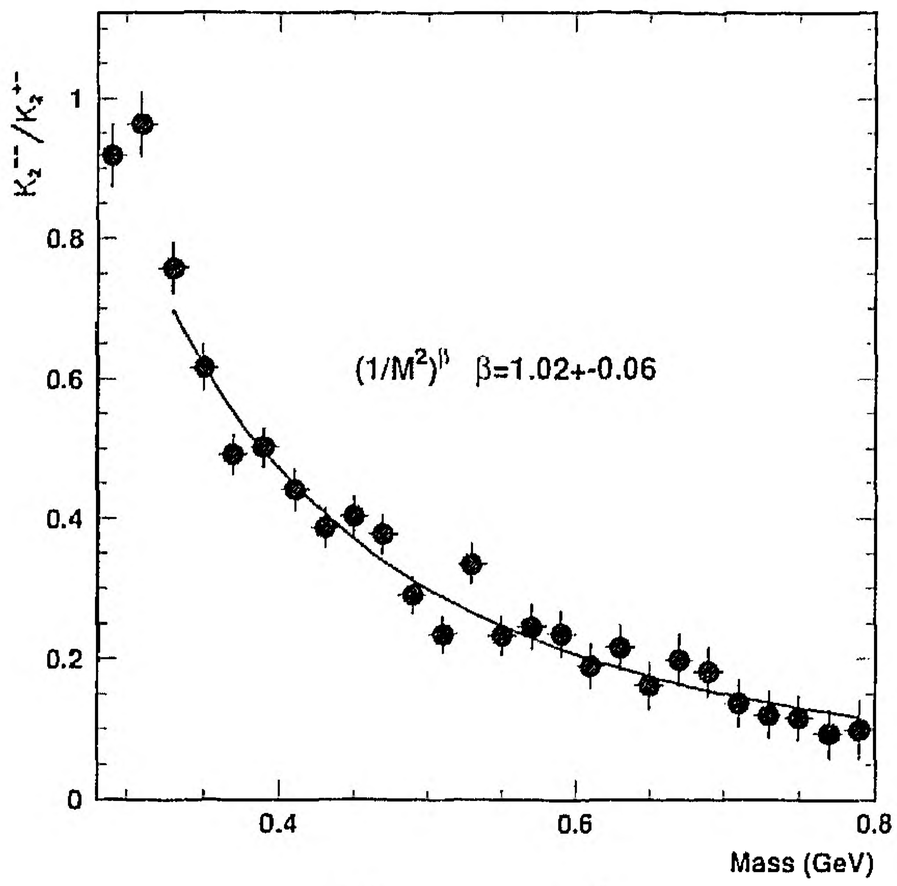

Fig. 4. The ratio of $K_2^{--}(M)$ and $K_2^{+-}(M)$ fitted by $A(1/M^2)^\beta$ (for $|y_i| < 2$)

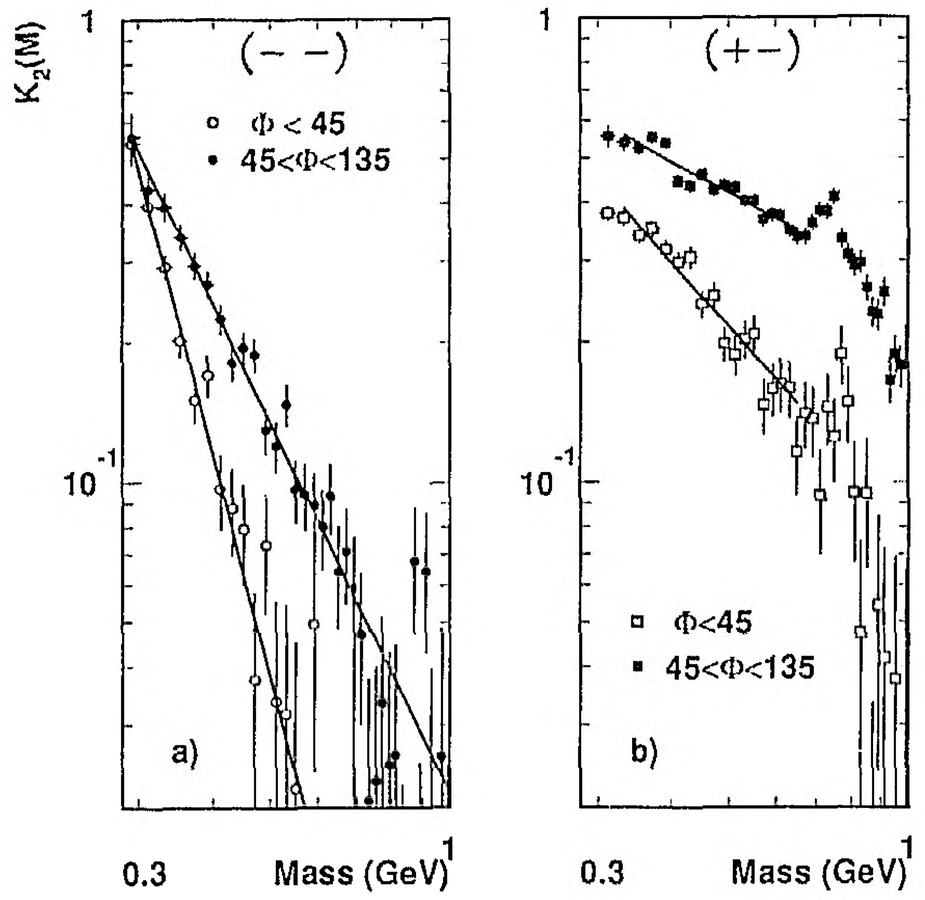

Fig. 6a, b. Normalised second-order factorial cumulants in intervals of relative azimuthal angle Φ. Lines are fits by $A(1/M^2)^\beta$ (see Table 1)

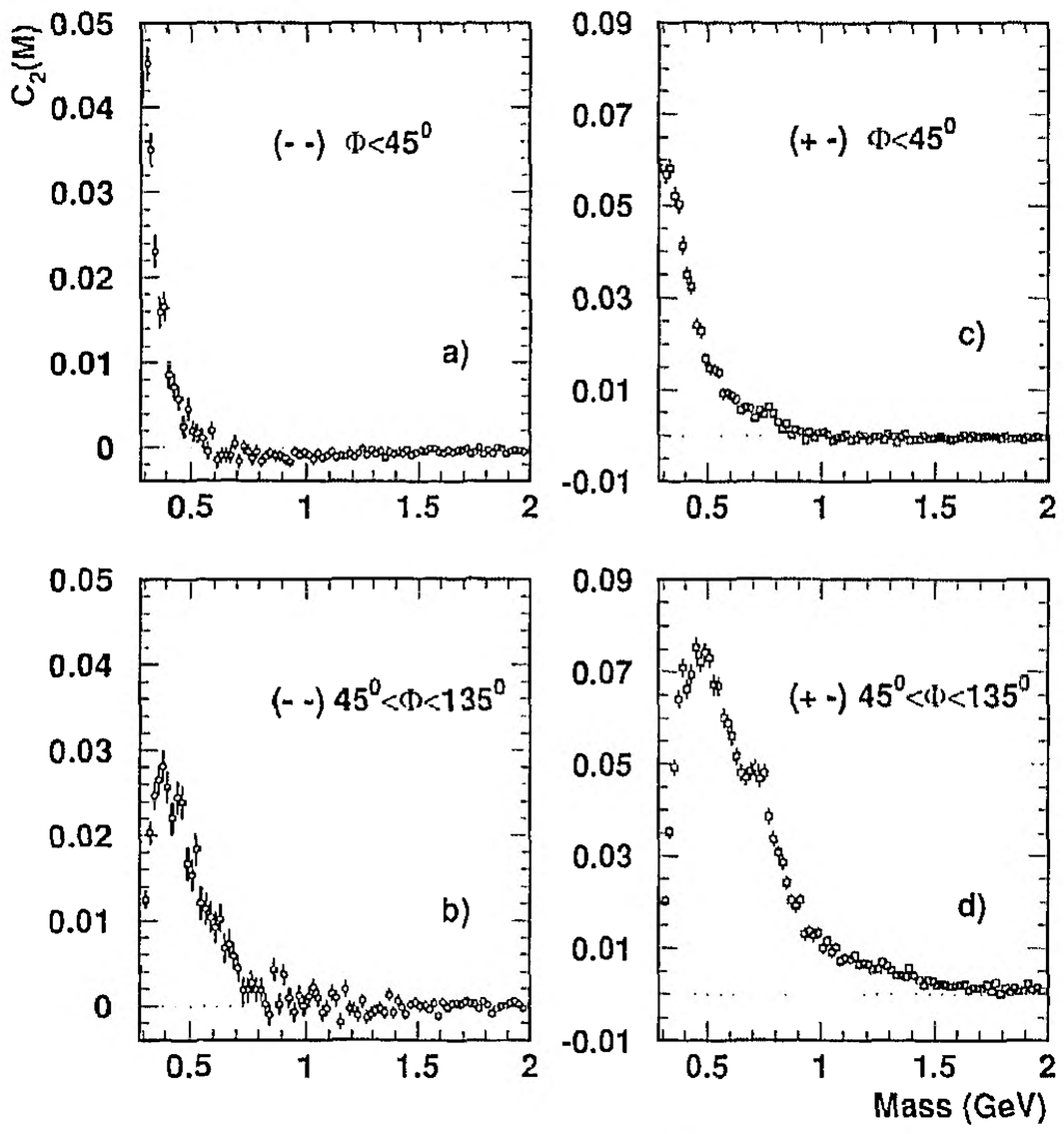

Fig. 5a–d. The correlation function $C_2^{--}(M)$ and $C_2^{+-}(M)$ in intervals of relative azimuthal angle Φ (in degrees)

The features shown by Fig. 5 are partly kinematical since small relative angles between the particle momenta favour small invariant mass. This kinematical effect equally affects $\rho_1 \otimes \rho_1(M)$. Dynamics is, therefore, better seen in $K_2(M, \Phi)$, displayed in Fig. 6 in a double-log scale. This function has the strongest M-dependence for $\Phi < 45°$. With this cut, also the ρ^0-signal is considerably reduced in $(+-)$-pairs. The lines are fits by (21) with parameters given in lines 6 and 7 of Table 1. We note, in particular, that $K_2^{--}(M)$ is power-behaved from threshold up to $\sim$1 GeV.

Figure 7a shows in more detail the dependence of K_2 on azimuthal angle for masses close to threshold, $M < 0.4$ GeV. $K_2^{--}(M)$ is nearly constant apart from some depletion in the interval $0 < \Phi < 30°$; $K_2^{+-}(M)$ rises gently to reach a nearly constant value for $\Phi > 80°$. The Φ-dependence is more pronounced in the interval $0.5 < M < 1$ GeV (Fig. 7b), in particular for $(+-)$-pairs.

From the data presented in this section, we conclude that the p_T-integrated normalised correlation function depends weakly on the azimuthal separation of the pair in the small-mass region, especially for like-charge combinations: the correlation function depends mainly on invariant mass. Both $K_2^{--}(M)$ and $K_2^{+-}(M)$ are power-behaved, the latter for $M < 0.6$ GeV.

3.3 Azimuthal angle dependence

In Fig. 5 we plot $C_2^{--}(M, \Phi)$ and $C_2^{+-}(M, \Phi)$ in various intervals of Φ, the angle between the transverse momenta of the pair.

Both for $(+-)$ and $(--)$ we observe a strong positive correlation at small M and small Φ, substantially narrower for $(--)$-pairs than for $(+-)$-pairs. The ρ^0 signal stands out more clearly for $45° < \Phi < 135°$ than in the other distribution.

3.4 Transverse momentum dependence

The observation by NA22 [15] that the intermittency effect is most pronounced for low-p_T particles (e.g. $p_T < 0.15$ GeV/c) and almost absent for larger p_T-values, has attracted much attention since it pointed to intermittency in hadron-hadron collisions as a "soft" effect. Low-p_T intermittency is also visible in the UA1 data [16] in spite of the bias against small p_T in this experiment. The reason for stronger intermittency remained rather

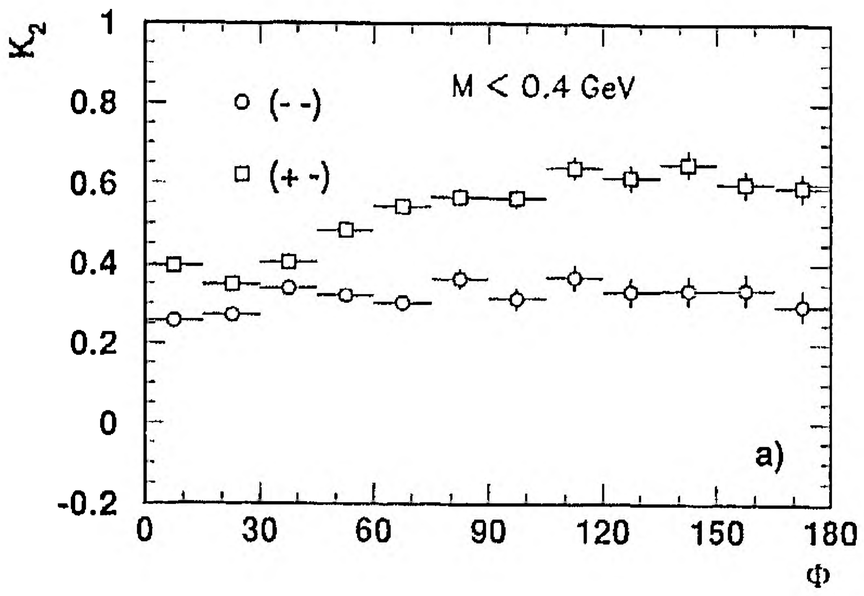

Fig. 7a, b. Normalised second-order factorial cumulants versus relative azimuthal angle for invariant masses **a** $M < 0.4$ GeV, **b** $0.5 < M < 1$ GeV

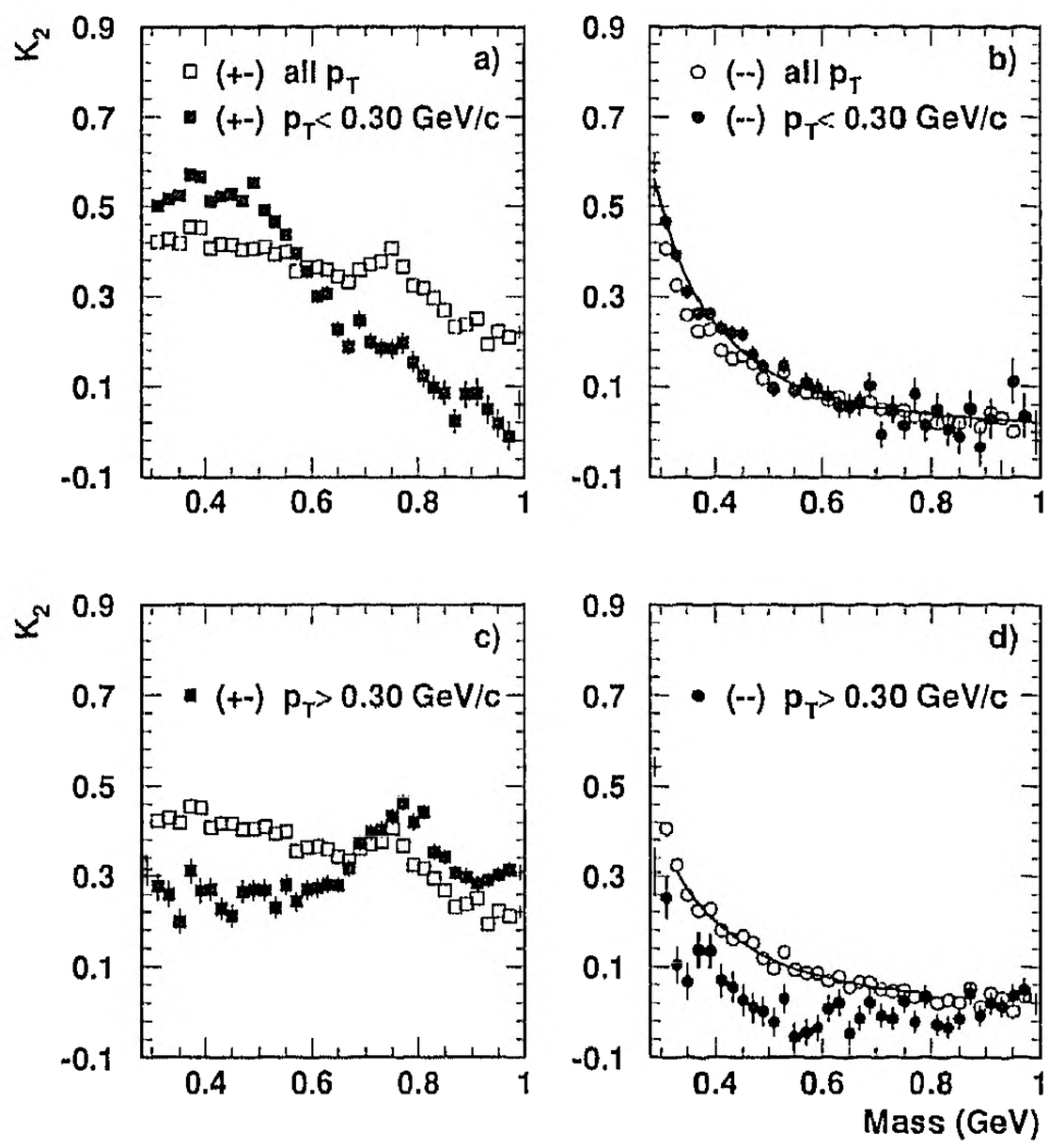

Fig. 9a–d. The normalised second-order factorial cumulants with restricted transverse momentum of the individual particles. Lines are fits by $A(1/M^2)^{\beta}$ (see Table 1)

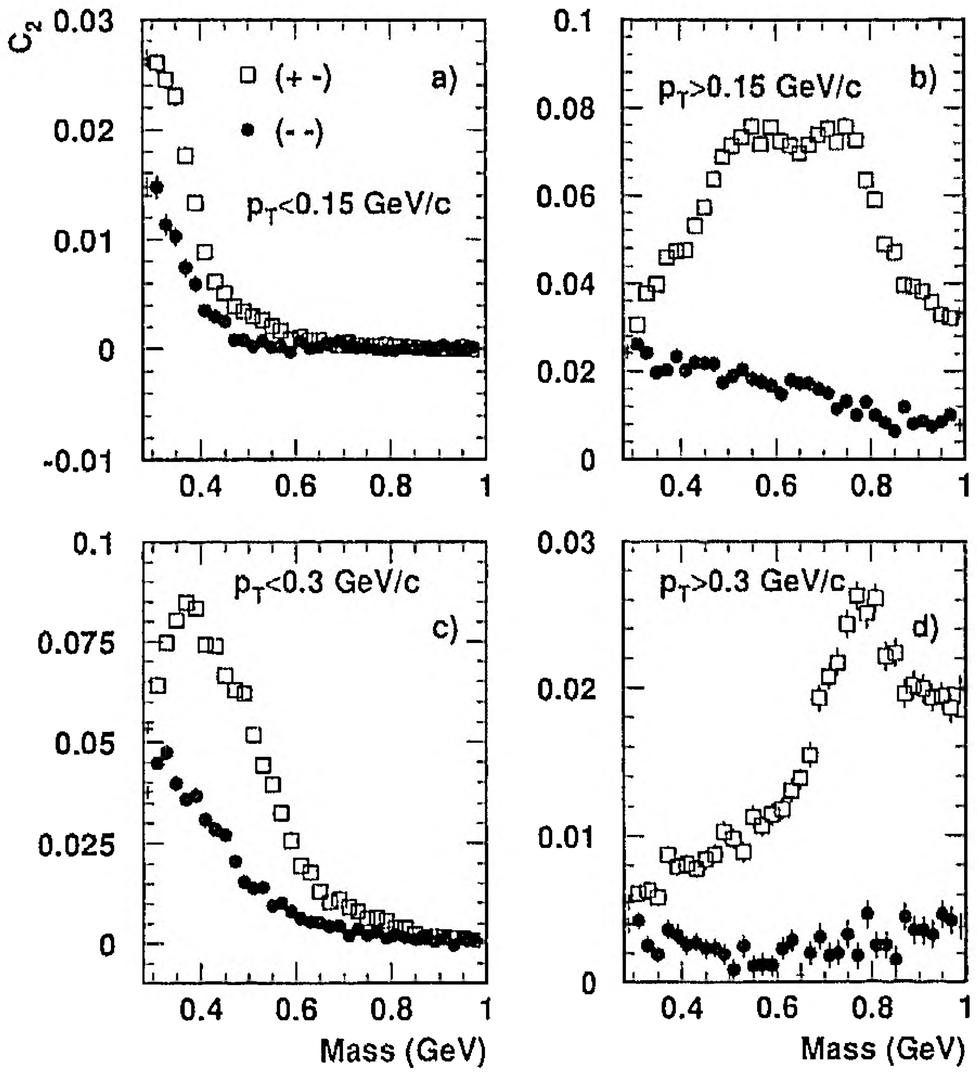

Fig. 8a–d. The correlation functions $C_2^{--}(M)$ and $C_2^{+-}(M)$ with restricted transverse momentum of the individual particles

unclear and, moreover, the effect could not be reproduced by presently used models.

To try and clarify this issue, we here study $C_2(M)$ and $K_2(M)$ in different intervals of transverse momentum. Figure 8 shows $C_2^{+-}(M)$ and $C_2^{--}(M)$ for particles with transverse momentum below and above 0.15 and 0.30 GeV/c, respectively.

For low-p_T particles (Fig. 8a, c), C_2 drops more rapidly to zero with increasing M than the all-p_T data (Fig. 2); $C_2^{--}(M)$ is zero, within errors, above 0.5 GeV. For $C_2^{+-}(M)$ this happens for $M \sim 0.7$–0.8 GeV. Note also that the otherwise prominent ρ^0-signal is nearly completely removed by the p_T-cut.

Imposing a lower limit on p_T (Figs. 8b, d) has the effect of enhancing the correlation at larger M and increases the influence of the ρ^0-meson. For $p_T > 0.3$ GeV/c, C_2^{--} is close to zero in the whole mass range studied ($M \leqq 1$ GeV).

As already hinted in Sect. 2.2, cuts on transverse momentum strongly influence the mass-spectra and C_2 for (trivial) kinematical reasons. Since this affects $\rho_2(M)$ and $\rho_1 \otimes \rho_1(M)$ alike, it is more instructive to consider the functions K_2. Examples of these are shown in Figs. 9a–d for $(+-)$- and $(--)$-pairs. For ease of comparison we also include the data for all p_T.

For $K_2^{+-}(M)$ (Fig. 9a), the selection $p_T < 0.3$ GeV/c eliminates most of the ρ^0-contribution; K_2 now has a much stronger dependence on M, compared to the all-p_T data. A likely explanation is that reflections from e.g. three-body resonance decays in the $(+-)$-channel are enhanced by the small-p_T cut. With $p_T > 0.3$ GeV/c (Fig. 9c), the ρ^0 stands out most prominently; the correlation function shows little M-dependence for $M < 0.6$ GeV.

From Fig. 9b, we note the interesting feature that $K_2^{--}(M)$ is hardly affected by the cut. This is also true for $p_T < 0.15$ GeV (not shown). For example, from a fit by the form (21) we find $\beta^{--} = 1.54 \pm 0.24$ and $\beta^{--} = 1.35 \pm 0.07$ for $p_T < 0.15$ GeV/c and

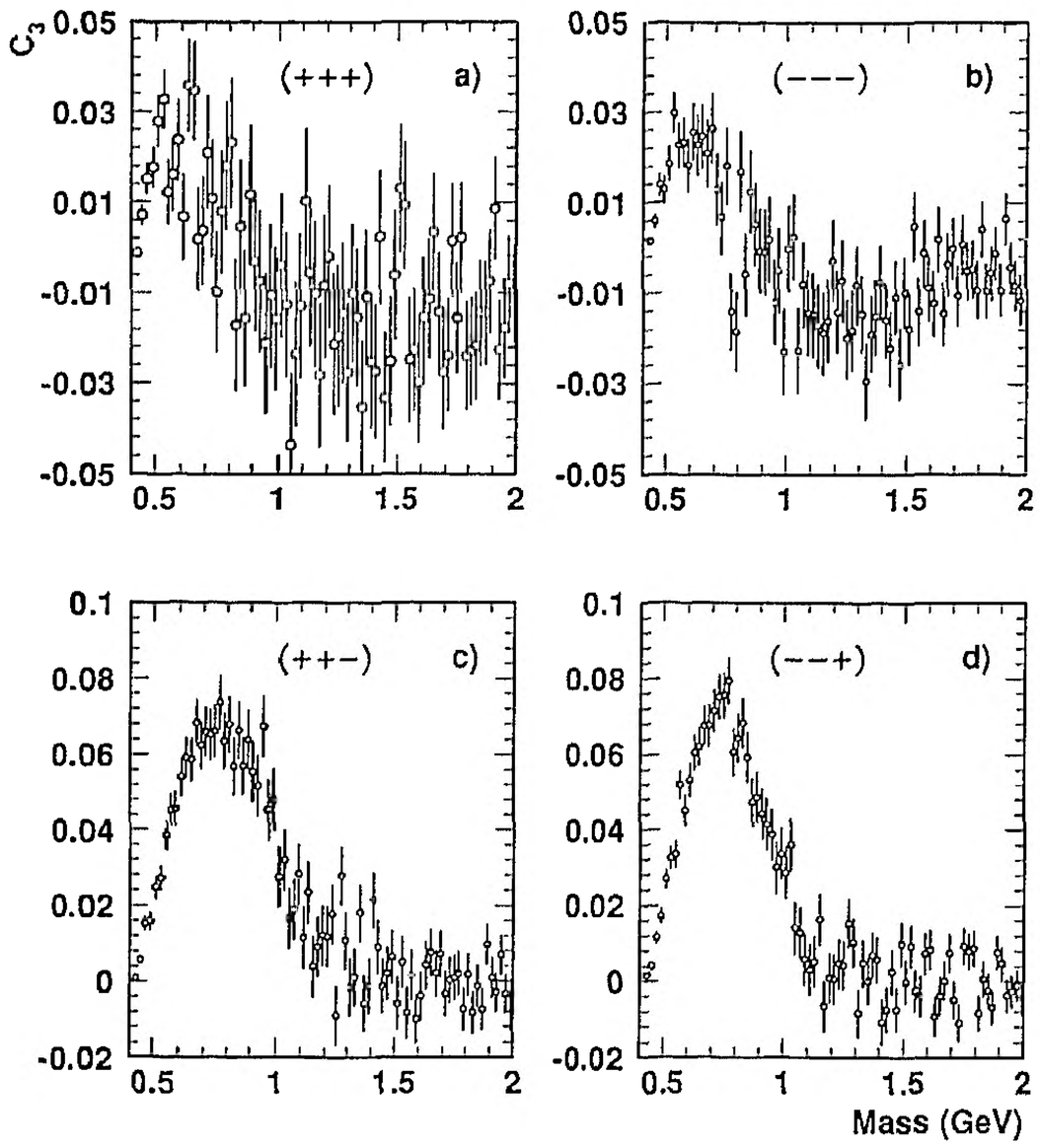

Fig. 10a–d. The third-order correlation function $C_3(M)$ for various charge combinations

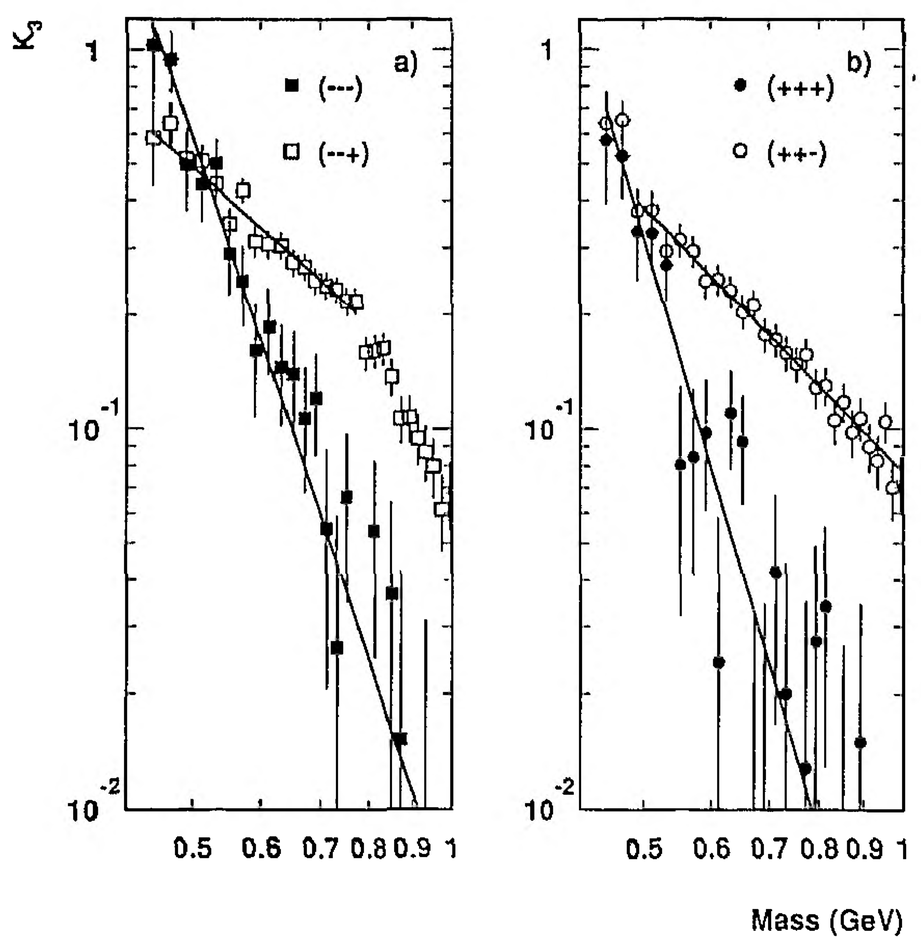

Fig. 11a, b. The third-order normalised factorial cumulant $K_3(M)$ for various charge combinations. Lines are fits by $A(1/M^2)^{\beta}$ (see Table 1)

$p_T > 0.15$ GeV/c, respectively, to be compared with $\beta^{--} = 1.29 \pm 0.04$ for all p_T (cf. Table 1). For $p_T > 0.3$ GeV/c, $K_2^{--}(M)$ is reduced in value for kinematical reasons.

We conclude that the two-particle correlation function of $(--)$-pairs* – a priori a function of five variables at fixed $\sqrt{s}$ – shows the strongest explicit dependence when studied in terms of the invariant-mass variable, at least in the small-mass region where intermittency is searched for.

The correlation function of unlike-charge pairs is influenced by direct-channel resonances and resonance reflections and is a more complicated function of the kinematical variables.

3.5 Three-particle cumulants

In Fig. 10 we present C_3, the third-order correlation function, as a function of the three-particle invariant mass. Non-exotic triples show a strong correlation below $M < 1.2$ GeV. For identical-particle triplets, errors are large, but a positive correlation is clearly seen for masses below 1 GeV.

The normalised cumulants K_3 are displayed in Fig. 11. The lines are power-law fits of the form (21) to the data with parameters given in Table 1. The $(---+)$-triplet data (Fig. 11a) exhibit an unexplained shoulder near 0.8 GeV, not seen in the charge-conjugate triplet (Fig. 11b). Nevertheless, cumulants of non-exotic triplets decrease as a power in $1/M^2$ with a slope $\beta \sim 1.0$–1.2, considerably faster than $(+-)$-pairs. Identical-particle triplets fall even steeper with M, with slopes of the order of 3.

4 Comparison to FRITIOF

The experimental study of factorial moments as a function of cell-size has revealed serious shortcomings in the Monte-Carlo generators commonly used to simulate multiparticle production processes. Discrepancies are largest between models* and data for hadron-hadron (and hA or AA) processes. For e^+e^- annihilations the generators based on JETSET [19–21] (or HERWIG [22, 23]) are much more successful. The reason why models which use essentially the same hadronisation algorithm (JETSET) for e^+e^- annihilation as for hh processes, fare so differently, still remains obscure.

In a previous study of rapidity correlations [24], serious disagreements of FRITIOF (and other models) with the data were reported. We have already mentioned that rapidity correlations are very insensitive to dynamical effects at small invariant mass and it is, therefore, not too surprising that the cause of the model failures remained unclear. In this section we show that analysis of correlations in terms of invariant mass not only confirms that FRITIOF – or rather JETSET – fails, but the method reveals specific deficiencies that need to be remedied. As will become clear, these are apparently not so much related to "new physics" but rather to a number of defects which have passed unnoticed.

We use FRITIOF, version 2, with parameter settings as described e.g. in [25]. We opt for this version – although more recent versions are now available – since it has been used in studies of many other topics in this

* This also holds for $(++)$-pairs not discussed here

* Here we consider the specific example of FRITIOF [17] but the same is true for e.g. the two-string dual parton model [18]

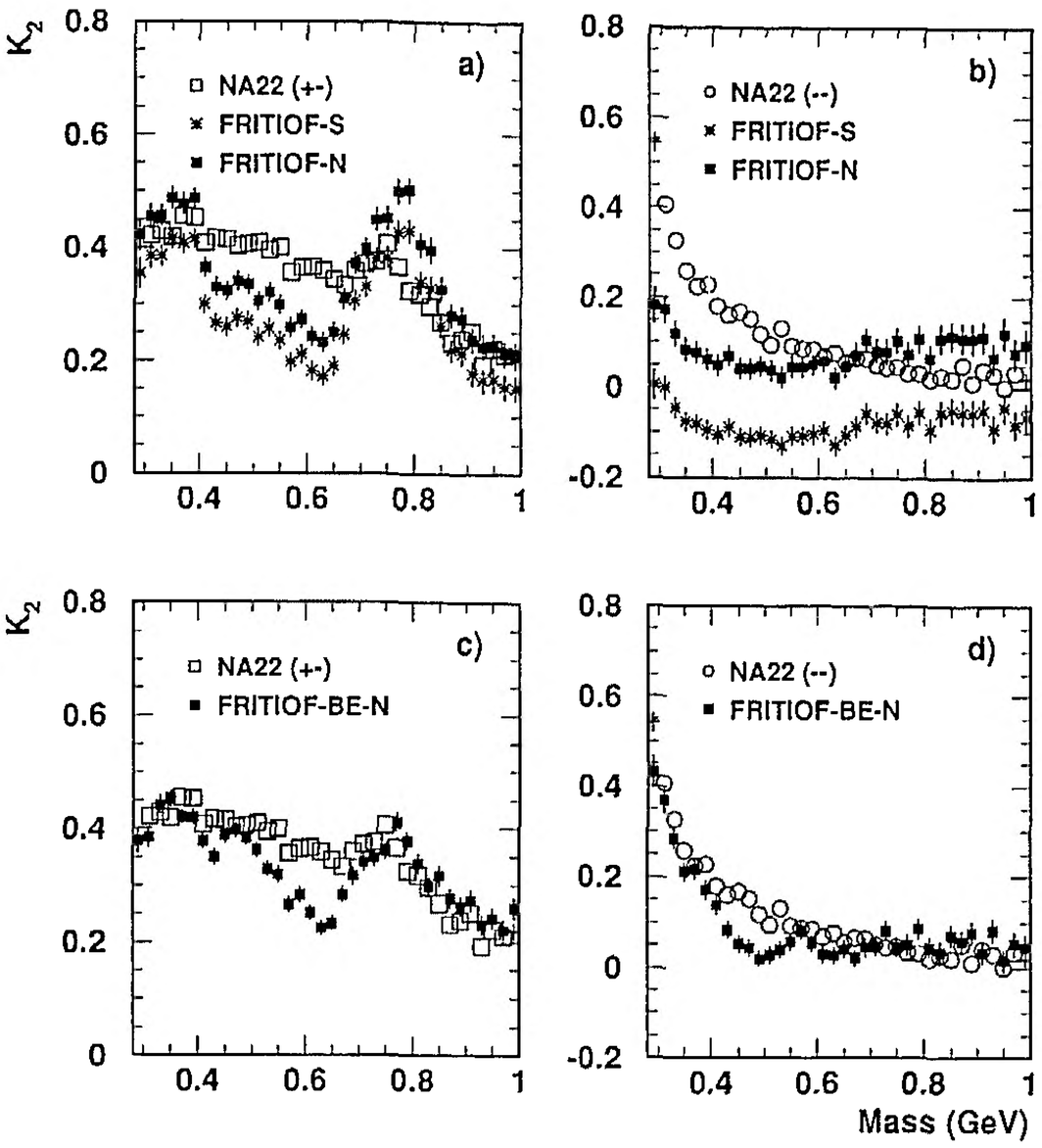

Fig. 12a–d. The normalised second-order factorial cumulant $K_2^{+-}(M)$ and $K_2^{--}(M)$ compared to FRITIOF 2. Predictions in **a–b** for FRITIOF and JETSET 6.3 with default parameters (FRITIOF-S) and renormalised (FRITIOF-N); **c–d** for FRITIOF rescaled, with Bose-Einstein enhancement and suppressed resonance production rates in JETSET

experiment. Since we are ultimately interested in a better understanding of the behaviour of factorial moment data, we limit the discussion to normalised factorial cumulants.

Figure 12a–b compares the data on $K_2^{+-}(M)$ and $K_2^{--}(M)$ to FRITIOF-S, the standard FRITIOF version with default NA22 parameters. The prediction for $K_2^{+-}(M)$ (Fig. 12a) bears little resemblance to the data: i) the predicted ρ^0-signal is too strong, ii) the correlation function falls much faster with M in the region below $M < 0.6$ GeV.

It is known that FRITIOF underestimates the width of the full phase-space (charged particle) multiplicity distribution or, equivalently, the second-order factorial cumulant, integrated over all M. To remove this global defect, we renormalized the FRITIOF predictions to the experimental values of K_2^{--} and K_2^{+-} for all M. The corresponding results are indicated as FRITIOF-N in Fig. 12. As to the structure in the region below $M = 0.6$ GeV, we find from FRITIOF that is due to reflections from η, η' and ω decays.

From previous NA22 studies, it is known that JETSET, with default parameters, overestimates the η production rate [25, 26] by as much as a factor of three. There are also indications from this and other experiments that the inclusive cross section of ρ^0 [27–30] and η' [31] is too large in JETSET by a similarly large factor. The influence on correlation functions and factorial moments of such deficiencies in the Monte Carlo's was not fully appreciated in earlier intermittency studies, with the exception of [32].

Figure 12b compares FRITIOF to $K_2^{--}(M)$ data. The predicted correlation (small and slightly negative in FRITIOF-S) is roughly constant in M, except for a peak at threshold which is related to η' decays. Unfortunately, the inclusive η' cross section is not directly measurable in this experiment. It is, therefore, impossible to assess the importance of its contribution to the strong rise of $K_2^{--}(M)$ seen in the data for M approaching the threshold. Still, if we assume that the η'-rate is overestimated by roughly the same amount as the η-rate, it becomes clear that another dynamical effect, present in the data but not in FRITIOF or JETSET, is responsible for the sharp decrease of $K_2^{--}(M)$ from threshold to $M \sim 0.6$ GeV.

A low-mass enhancement of the type seen in Fig. 12b is, of course, expected from Bose-Einstein interference. By this we mean small-mass enhancements which are the consequence of symmetrisation of production amplitudes. These include interferences between "prompt" production amplitudes, as well as those between "prompt"- and resonant final-state interactions. The net effect of all these is obviously difficult to estimate without a detailed model calculation at the amplitude level. Simplified treatments can be found in [13, 8] (see also [33]). In general such calculations predict strong enhancements of the correlation function at very small masses. Under the (extremely naive) assumption that pions are emitted from a production volume with an extension of the order of the pion Compton wavelength (1.4 fm) without suffering any interaction – hardly likely in a strong interaction process – one would expect to observe a Bose-Einstein effect from threshold up to about 0.4–0.5 GeV.

To assess the importance of (naive) Bose-Einstein correlations, we have incorporated in FRITIOF such an enhancement, using the algorithm developed by Sjöstrand for JETSET 7.3 [34, 35]. We use an exponential parametrisation in $|Q|$:

$$\mathrm{BE}(M) = 1 + \lambda \mathrm{e}^{-R|Q|}, \tag{22}$$

with $\lambda = 0.5$ and $R = 0.8$ fm.

Furthermore, to appreciate the influence of pseudoscalar and vector mesons, we have introduced ad hoc modifications* in JETSET which reduce the ρ^0 (η and η') production rate to 1/2 (1/3) of the "default" rate.

The results, indicated as FRITIOF-BE-N, are shown in Figs. 12c, d. For $K_2^{+-}(M)$, agreement is acceptable in and above the ρ^0-region and below $M < 0.5$ GeV, but not in the intermediate mass region. For $K_2^{--}(M)$, FRITIOF agrees with the data (after global renormalisation, see before) for $M > 0.6$ GeV. Nevertheless, the M-dependence remains too strong in the region around 0.5 GeV.

We should stress that the value of λ, which determines the strength of the BE-effect, is rendered quite uncertain by the unknown contribution from η', as discussed earlier. With this caveat, we are tempted to conclude that a

* One should note that such a "brute-force" procedure is hardly acceptable in the framework of the LUND fragmentation picture and is likely to adversely affect agreement with other observables which are otherwise well described

BE-effect of a "traditional" form (22) could explain the enhancement of $K_2^{--}(M)$ for $M \leqq 0.4$ but the remaining deviations require further study.

For three-particle correlations, the FRITIOF predictions for $C_3(M)$ (not shown) are close to zero for all values of M, contrary to the data.

In summary, we learn from the FRITIOF calculations that the model's difficulties in reproducing the measured correlation functions are to a large extent caused by i) incorrect production rates of (at least) ρ^0, η, and, possibly ω and η' mesons, ii) the absence of a Bose-Einstein small-mass enhancement mechanism.

Whether there is evidence for "new physics" in the data is difficult to judge at present. It remains to be seen if the most obvious deficiencies in particle and resonance production rates can be cured in a consistent manner in models such as JETSET. The apparent success of the Parton-Shower + JETSET Monte-Carlo in e^+e^- annihilations most likely means that correlations are less sensitive to resonance and Bose-Einstein effects at LEP energies or, that the model parameters are tuned to the data in a way which compensates for the deficiencies.

5 Discussion and conclusions

In this paper we have studied two- and three-particle correlations in various charge combinations in terms of the invariant mass of pairs and triplets. This work was motivated by the recently revived interest in correlation phenomena, and, in particular, the considerable experimental and theoretical effort invested in the search for intermittency and fractal dynamics.

The work on intermittency initially concentrated on the behaviour of factorial moments of the charged multiplicity distribution in progressively decreasing intervals of rapidity. This geometric "box-counting" approach, familiar in fractal theory, was soon extended to two- and three-dimensional phase space. Due to the highly non-uniform particle population, such analyses necessitated the use of variable transformations [36, 37] which considerably complicated interpretation of the results in terms of known dynamical effects and experimental bias.

With the "correlation integral" technique [12], the emphasis returned to correlation measurements in terms of suitably defined inter-particle distances. This avoided the arbitrariness in the choice of geometrical volume and its subdivisions, inherent to the previous analysis methods. In present applications [38, 39], Lorentz-invariant distance measures such as Q^2 have proven to be most revealing. It is worthwhile to stress that cumulative, rather than differential quantities are studied with this technique, again inspired by fractal theory.

In this paper, we analysed differential distributions. The (apparent) loss in statistical accuracy, compared to cumulative quantities, is amply compensated by greater sensitivity to fine-structure.

The data presented here help in clarifying several aspects of earlier factorial moment analyses.

- The factorial cumulants $K_2(M)$ and $K_3(M)$ behave as powers in $(1/M^2)$ from threshold to ~ 1 GeV in invariant mass. This confirms earlier speculations [40, 6] that normalised correlation functions, rather than inclusive densities might show scale-invariance.
- Factorial cumulants of "exotic" particle combinations show the strongest dependence on invariant mass. For "non-exotic" combinations, such as $(+-)$-pairs, the M-dependence is much weaker. Moreover, it is sensitive to the kinematical region examined and clearly related to resonances occurring in this channel.
- "All-charged" data mix very different dynamics and should be interpreted with caution.
- For small masses, the function $K_2^{\pm\pm}$, depends weakly on the transverse momentum of the particles and on their relative azimuthal angle, and is mainly a function of invariant mass. This fact explains [41] why selection of low-p_T particles gives rise to *enhanced* intermittency in rapidity-space [15] but *weaker* intermittency in terms of correlation integrals [38], two, at first sight, contradictory conclusions.
- The much larger powers β for like-sign than for unlike-sign pairs and triplets mean that the intermittency effect is predominantly due to the former. Bose-Einstein type correlations are a natural candiate to explain this difference. Accepting this hypothesis, we conclude from our data that the BE-effect leads to normalised correlation functions which are power-behaved in $(1/M^2)$. This is at variance with the traditionally adopted parametrisation of the two-particle *density* in terms of Gaussians or exponentials in Q^2 with parameters related to interaction-volume dimensions and wavefunction coherence. However, it is easy to verify that a function of the type (22), expressed in terms of invariant mass is, with present accuracy, almost indistinguishable from a function of the form $1 + A(1/M^2)^\beta$ as suggested by the power law (21). As a result, and depending on the point of view taken, present BE-data can be used either as evidence for scale-invariance of K_2 in the invariant mass variable, or as a confirmation of the traditional BE-interpretation.
- The origin of the failures exhibited by models such as FRITIOF, is most clearly revealed in our analysis. These failures are not necessarily due to "novel" dynamics, absent (by definition) in the models. They are in first instance a consequence of a variety of defects – such as incorrect resonance production rates and absence of identical particle symmetrisation – which belong to "standard" hadronisation phenomenology. Still, these defects are not easy to cure in a consistent manner by simple parameter-tuning and "new" physics may be needed to restore internal consistency in e.g. string-fragmentation models of the LUND type. Indeed, present work [42] on this subject starts to provide hints that a purely probabilistic treatment of the break-up of colour fields might have to be supplemented with new mechanisms, somehow related to the chiral structure of the non-perturbative QCD vacuum.
- Originating mainly from the low invariant-mass region (typically < 1.5 GeV), it is not impossible that the observed correlations, being dominated by strong final-state interactions, are quite independent of the process

initiating the primary colour separation in the collision. This would explain "universality" in the sense discussed earlier.

● Many authors argue that "intermittency" is somehow connected to (nearly scale-invariant) perturbative QCD-cascading. Others strongly contest this view on the argument that QCD cascades have a limited extent even at LEP energies and are dominated by a very small number of "hard" emissions. In the former case, one may expect significant differences in the correlation functions at low mass for e^+e^-, on the one hand, and for hh, hA and AA collisions, on the other hand. Whatever the final outcome, if differences are found, they should be used to clarify the respective roles of perturbative and hadronisation phases in the different types of collision processes.

Acknowledgements. It is a pleasure to thank the EHS coordinator L. Montanet and the operating crews and staffs of EHS, SPS and H2 beam, as well as the scanning and processing teams of our laboratories for their invaluable help with this experiment. We are grateful to III. Physikalisches Institut B, RWTH Aachen, Germany, DESY-Institut für Hochenergiephysik, Zeuthen, Germany, Department of High Energy Physics, Helsinki University, Finland for early contributions to this experiment. We thank the Nederlandse Organisatie voor Wetenschappelijk Onderzoek (NWO) for support of this project within the program for subsistence to the former Soviet Union (07-13-038).

References

1. W.A. Zajc: Proc. Int. Workshop on Correlations and Multiparticle Production, Marburg, p. 439, M. Plümer, S. Raha, R.M. Weiner (eds.). Singapore: World Scientific 1991
2. St. Macellini: Proc. Joint Int. Lepton-Photon Symp. and Europhys. Conf. on High Energy Physics, V. I, p. 750, S. Hegarty et al. (eds.). Singapore: World Scientific 1992; B. De Lotto: Udine preprint 92/10/BL; Proc. XXVI Int. Conf. on High Energy Physics, Dallas, USA, 1992, J.R. Sanford (ed.). AIP Conference Proc. no. 272, p. 955
3. A. Białas, R. Peschanksi: Nucl. Phys. B273 (1986) 703
4. A. Białas, R. Peschanski: Nucl. Phys. B308 (1988) 857
5. E.A. De Wolf, I.M. Dremin, W. Kittel: Nijmegen preprint HEN-362 (1993); Brussels preprint IIHE-ULB-VUB-93-01, to be publ. in Phys. Rep. C
6. K. Fiałkowski: Phys. Lett. B272 (1991) 139; idem: in: Proc. Ringberg Workshop on Multiparticle Production, p. 238, R.C. Hwa, W. Ochs, N. Schmitz (eds.). Singapore: World Scientific 1992
7. E.L. Berger, R. Singer, G.H. Thomas, T. Kafka: Phys. Rev. D15 (1977) 206
8. G.H. Thomas: Phys. Rev. D15 (1977) 2636
9. M. Adamus et al., NA22 Coll.: Z. Phys. C32 (1986) 475
10. M. Adamus et al., NA22 Coll.: Z. Phys. C39 (1988) 311
11. A.H. Mueller: Phys. Rev. D4 (1971) 150
12. P. Lipa, P. Carruthers, H.C. Eggers, B. Buschbeck: Arizona preprint AZPHTH/91-53
13. P. Grassberger: Nucl. Phys. B120 (1977) 231
14. I.V. Ajinenko et al., NA22 Coll.: Z. Phys. C58 (1993) 357
15. I.V. Ajinenko et al., NA22 Coll.: Phys. Lett. B261 (1991) 165
16. B. Buschbeck, UA1 Coll.: Festschrift L. Van Hove, p. 211, A. Giovannini, W. Kittel. Singapore: World Scientific 1990
17. B. Andersson, G. Gustafson, B. Nilson-Almqvist: Nucl. Phys. B281 (1987) 289
18. A. Capella: in Proc. Europ. Study Conf. on Protons and Soft Hadronic Int., Erice, p. 199, R.T. Van de Walle (ed.). Singapore: World Scientific 1982; E.A. De Wolf: in Proc. XV Int. Symp. on Multiparticle Dynamics, Lund, Sweden 1984, p. 1. G. Gustafson, C. Peterson. Singapore: World Scientific 1984
19. T. Sjöstrand: Comput Phys. Commun. 39 (1986) 347
20. M. Bengtsson, T. Sjöstrand: Comput. Phys. Commun. 43 (1987) 367
21. M. Bengtsson, T. Sjöstrand: Nucl. Phys. B289 (1987) 810
22. G. Marchesini, B. Webber: Nucl. Phys. B310 (1988) 461
23. G. Marchesini, B. Webber: Cavendish-HEP-88/7 (1988)
24. I.V. Ajinenko et al., NA22 Coll.: Z. Phys. C51 (1991) 167
25. M.R. Atayan et al., NA22 Coll.: Z. Phys. C54 (1992) 247
26. P.D. Acton et al., OPAL Coll.: Phys. Lett. B305 (1993) 407
27. N.M. Agababyan et al., NA22: Z. Phys. C46 (1990) 387
28. C.T. Jones et al., WA21 Coll.: Z. Phys. C51 (1991) 11
29. W.D. Walker et al.: Phys. Lett. B255 (1991) 155
30. H. Albrecht et al., ARGUS Coll.: DESY preprint 93-083 (1993)
31. D. Buskelic et al., ALEPH Coll.: Phys. Lett. B292 (1992) 210
32. G. Gustafson, C. Sjögren: Phys. Lett. B248 (1990) 430
33. M. Gyulassy, S.K. Kauffmann, L.W. Wilson: Phys. Rev. C20 (1979) 2267
34. T. Sjöstrand: Comput. Phys. Commun. 27 (1982) 243
35. T. Sjöstrand, M. Bengtsson: Comput. Phys. Commun. 43 (1987) 367
36. W. Ochs: Phys. Lett. B247 (1990) 101; Z. Phys. C50 (1991) 339
37. A. Białas, M. Gazdzicki: Phys. Lett. B252 (1990) 483
38. N. Agababyan et al., NA22 Coll.: Z. Phys. C59 (1993) 405
39. F. Mandl, B. Buschbeck, DELPHI/UA1 Coll.: Proc. XXII Int. Symp. on Multiparticle Dynamics, Santiago de Compostela, Spain, 1992, p. 561. A. Pajares (ed.). Singapore: World Scientific
40. H.C. Eggers: PhD. Thesis, Univ. of Arizona, 1991
41. E.A. De Wolf: in: Proc. XXII Int. Symp. on Multiparticle Dynamics, Santiago de Compostela, Spain, 1992, p. 263, A. Pajares (ed.). Singapore: World Scientific
42. G. Gustafson: talk at Cracow Workshop on Soft Physics and Fluctuations, Cracow 1993, to be published; B. Andersson, G. Gustafson: private communication

Z. Phys. C 61, 567–577 (1994)

ZEITSCHRIFT
FÜR PHYSIK C

Invariant mass dependence of particle correlations in $\pi^+ p$ and $K^+ p$ interactions at 250 GeV/c

EHS/NA22 Collaboration

I.V. Ajinenko[5], F. Botterweck[4,a], M. Charlet[4,b], P.V. Chliapnikov[5], E.A. De Wolf[1,c], K. Dziunikowska[2,d], A.M.F. Endler[6], Z.G. Garutchava[7], G.R. Gulkanyan[8], J.K. Karamyan[8], D. Kisielewska[2,d], W. Kittel[4], F.K. Rizatdinova[3], E.K. Shabalina[3], L.N. Smirnova[3], A. Tomaradze[7,e], F. Verbeure[1]

[1] Department of Physics, Universitaire Instelling Antwerpen, B-2610 Wilrijk and Inter-University Institute for High Energies, B-1050 Brussels, Belgium
[2] Institute of Physics and Nuclear Technique of Academy of Mining and Metallurgy and Institute of Nuclear Physics, PL-30055 Krakow, Poland
[3] Nucl. Phys. Institute, Moscow State University, 119899 Moscow, Russia
[4] University of Nijmegen and NIKHEF-H, NL-6525 ED Nijmegen, The Netherlands
[5] Institute for High Energy Physics, 142284 Protvino, Russia
[6] Centro Brasileiro de Pesquisas Fisicas, 22290 Rio de Janeiro, Brazil
[7] Institute of High Energy Physics of Tbilisi State University, 380086 Tbilisi, Georgia
[8] Institute of Physics, 375036 Yerevan, Armenia

Received 11 October 1993

Abstract. We study two- and three-particle correlations as a function of invariant mass. Using data on $\pi^+ p$ and $K^+ p$ collisions at 250 GeV/c, we compare correlation functions and normalised factorial cumulants for various charge combinations. Strong positive correlations are observed only at small invariant masses. The normalised cumulants for "exotic" $[(--), (++)]$ and "non-exotic" pairs $(+-)$ and triplets decrease in power-like fashion with increasing invariant mass. The mass dependence is not incompatible with the power-law behaviour as expected in a Dual Mueller-Regge framework. Comparison with FRITIOF reveals strong disagreements, which are due to too large production rates of resonances, such as ρ^0 and η, and the absence of a Bose-Einstein low-mass enhancement in JETSET.

1 Introduction

For many years, correlations among hadrons produced in high-energy multi-particle processes have been studied in a variety of variables. Of obvious importance are analyses of multiparticle spectra in terms of the invariant mass of two- and more particle systems, which allowed identification of hadronic resonances.

Studies of correlations in rapidity have helped to establish the fruitful concept of short-range order in momentum space, a dynamical property already present in the earliest multiperipheral pictures of particle production, later extended to ladder diagrams with Regge exchanges. In these, propagators are functions of nearest-neighbour invariant-masses which, at high energy and large mass, are conveniently expressed in terms of rapidity distances.

Correlations attributed to Bose-Einstein symmetrisation of identical boson amplitudes have been much discussed in the literature (for recent reviews see [1, 2]). They are often studied in terms of the difference of particle-pair four-momenta, a traditional choice being $Q_{ij}^2 = -(q_i - q_j)^2$.

Recently, correlation studies have attracted renewed attention in connection with the search for self-similar particle-density fluctuation phenomena, commonly known as "Intermittency" [3, 4]. Intermittency means that the normalised factorial moments F_q of the multiplicity distribution in a phase-space volume δ are power-behaved

$$F_q(\delta) \propto \delta^{-\phi_q}, \quad (\phi_q > 0) \tag{1}$$

over a range of scales, down to the experimental resolution. This further implies that the q-particle densities and correlation functions are singular in the limit $\delta \to 0$. The present status of this field is reviewed in [5].

A significant step towards better understanding of the physics behind intermittency was made by Fiałkowski [6]. Using data in three-dimensional phase space on μp, π/Kp, pA and AA collisions, he noted that F_2 shows a

[a] Now at Universitaire Instelling Antwerpen
[b] EC Guest Scientist
[c] Onderzoeksleider NFWO, Belgium
[d] Partially supported by grants from CPBP 01.06 anf 01.09
[e] Also at Universitaire Instelling Antwerpen

surprisingly high degree of "universality". Writing $F_2(\delta)$ as

$$F_2(\delta) = A + B\delta^{-\phi_2}, \tag{2}$$

ϕ_2 was found to be around 0.4–0.5 in all processes considered. The B-values also turn out to be quite similar. The author, therefore, speculated that intermittency may be a "universal collective" effect.

As remarked in [6], δ in (2) is related, albeit non-uniquely, to Q^2 or $M = \sqrt{Q^2 + 4\mu^2}$, the invariant mass of the particle pairs (μ is the pion mass). The functional form of (2) would then mean that the normalised two-particle cumulant K_2 is power-behaved in M or in Q^2. The latter is singular at $Q^2 = 0$, while the former remains finite at threshold. This argument suggests that it may be rewarding to study correlation functions and factorial moments directly in terms of invariant mass. This is the subject of the present paper.

The idea to study correlations as a function of invariant-mass was, to our knowledge, first used in [7]. This analysis was based on low statistics pp data at 205 GeV/c. It demonstrated that the factorial cumulant $K_2 \equiv F_2 - 1$ (see further below) follows an approximate power law with very different powers for like-charge ("exotic") and unlike-charge ("non-exotic") hadron pairs. In [7] this is written as:

$$K_2(M) \propto (M^2)^{\alpha_X(0)-1}. \tag{3}$$

The notation reminds of the interpretation of (3) in terms of the Mueller-Regge formalism. The power $\alpha_X(0)$ is the appropriate Regge-intercept; $X = R$ for non-exotic pairs and $X = E$ for exotic ones. The ratio K_2^{--}/K_2^{+-} was further seen to fall as M^{-2}, consistent with $\alpha_R(0) - \alpha_E(0) = 1$. Not relying on Mueller-Regge theory, the authors argued that most of the correlations at small M are due to resonance decays into three or more pions and to interference of amplitudes [8].

In this paper we study the invariant-mass dependence of two- and three-particle correlations in a combined sample of $\pi^+ p$ and $K^+ p$ interactions at $\sqrt{s} = 22$ GeV. The experimental procedure and the formalism used are described in Sect. 2. Results and their implications for intermittency are discussed in Sect. 3. The data are compared to the Lund FRITIOF model for hadron-hadron interactions in Sect. 4. Conclusions and a summary are given in Sect. 5.

2 Experimental procedure

2.1 Event selection

In this CERN experiment, the European Hybrid Spectrometer (EHS) is equipped with the Rapid Cycling Bubble Chamber (RCBC) as an active vertex detector and exposed to a 250 GeV/c tagged positive, meson enriched beam. In data taking, a minimum bias interaction trigger is used. The details of the spectrometer and the trigger can be found in previous publications [9, 10].

Charged particle tracks are reconstructed from hits in the wire- and drift-chambers of the two lever-arm magnetic spectrometer and from measurements in the bubble chamber. The average momentum resolution $\langle \Delta p/p \rangle$ varies from a maximum of 2.5% at 30 GeV/c to around 1.5% above 100 GeV/c.

Events are accepted for the analysis when measured and reconstructed charge multiplicity are the same, charge balance is satisfied, no electron is detected among the secondary tracks and the number of reconstructed tracks rejected by our quality criteria is at most 0, 1, 1, 2 and 3 for events with charge multiplicity 2, 4, 6, 8 and > 8, respectively. Losses of events during measurement and reconstruction are corrected for using the topological cross sections [9]. Elastic events are excluded. Furthermore, an event is called single-diffractive, and excluded from the sample, if the total charge multiplicity is smaller than 8 and at least one of the positive tracks has $|x_F| > 0.88$. After these cuts, we remain with a sample of inelastic non-single-diffractive $\pi^+/K^+ p$ interactions consisting of 114 472 events. The results presented below pertain to the combined $\pi^+ p$ and $K^+ p$ samples.

For momenta $p_{\mathrm{LAB}} < 0.7$ GeV/c, the range in the bubble chamber and/or the change of track curvature is used for proton identification. In addition, a visual ionization scan has been used for $p_{\mathrm{LAB}} < 1.2$ GeV/c on the full $K^+ p$ and 62% of the $\pi^+ p$ sample. Positive particles with $p_{\mathrm{LAB}} > 150$ GeV/c are given the identity of the beam particle. Other particles with momenta $p_{\mathrm{LAB}} > 1.2$ GeV/c are not identified in the present analysis and are treated as pions. Identified protons are removed from the track sample.

2.2 The correlation function in invariant mass

The two-particle correlation function for hadrons a and b (assumed to be pions in the following) is defined as the inclusive coincidence rate per collision, minus the rate expected for uncorrelated hadrons a and b:

$$C_2^{ab}(q_1, q_2) \equiv \rho_2^{ab}(q_1, q_2) - \rho_1^a(q_1)\,\rho_1^b(q_2). \tag{4}$$

In this expression $q_i(p_i, E_i)$, $(i = 1, 2)$, are the four-momenta of the two hadrons. The invariant two-particle inclusive density is

$$\rho_2^{ab}(q_1, q_2) = \frac{E_1 E_2}{\sigma_I} \frac{\mathrm{d}\sigma}{\mathrm{d}^3 p_1\, \mathrm{d}^3 p_2}. \tag{5}$$

The invariant single-particle inclusive density is

$$\rho_1^{a,b}(q) = \frac{E}{\sigma_I} \frac{\mathrm{d}^3\sigma}{\mathrm{d}^3 p}, \tag{6}$$

with σ_I the inelastic cross section. The densities (5–6) are normalised as follows

$$\iint \rho_2(q_1, q_2) \frac{\mathrm{d}^3 p_1}{E_1} \frac{\mathrm{d}^3 p_2}{E_2} = \langle n_a (n_b - \delta_{ab}) \rangle, \tag{7}$$

$$\int \rho_1^{a,b}(q) \frac{\mathrm{d}^3 p}{E} = -\langle n_{a,b} \rangle, \tag{8}$$

with $\delta_{ab}=1$ if particles a and b are of the same type, and $\delta_{ab}=0$ otherwise. The integrations and the averages are taken over full or part of phase space.

The function C_2 in (4) depends on six dependent variables, a common choice being the c.m. energy, $\sqrt{s}$, the c.m. rapidities y_1 and y_2, the magnitudes p_{T_1}, p_{T_2}, the transverse momenta, and their relative azimuthal angle, Φ.

Most often, measurements of C_2 average over the transverse degrees of freedom, leaving only the longitudinal momentum (p_L) or rapidity dependence. The resulting correlation function is

$$C_2^{ab}(y_1, y_2)=\int \mathrm{d}^2 p_{T_1} \int \mathrm{d}^2 p_{T_2}\, C_2^{ab}(q_1, q_2)\,. \tag{9}$$

It is important to note that any structure which occurs at fixed invariant mass M ($M^2=(q_1+q_2)^2$), due e.g. to resonances or resonance reflections, is in general smeared out in the integrated correlation function (9). In fact, $C_2(y_1, y_2)$ depends mainly on the angular decay of the system and much less so on the mass spectrum. For isotropic decay it has the familiar approximately Gaussian shape.

Here, we are interested in correlation effects in invariant mass near threshold and shall, therefore, keep M (or Q^2, see below) in the set of independent variables describing C_2. We further keep p_{T_1}, p_{T_2} and Φ in the set and average over the longitudinal momentum of the system with mass M. The relation between M and $\Delta y=y_1-y_2$ is

$$M^2=2\mu^2-2\,p_{T_1}p_{T_2}\cos\Phi+2\,m_{T_1}m_{T_2}\cosh\Delta y\,, \tag{10}$$

with $m_T^2=\mu^2+p_T^2$. For large M and large Δy, one has

$$M^2\sim\exp(|\Delta y|)\,. \tag{11}$$

However, for small M or small Δy, relevant in intermittency studies, the relation between these variables is greatly influenced by the values of the transverse momenta. From (10) one also sees that selection of particles with small transverse momentum will introduce a shift towards small values in the invariant mass distribution integrated over Φ.

When (4) is integrated over the p_{T_1}, p_{T_2} and Φ, and over the longitudinal momentum of the pair, C_2 becomes a function only of M, at fixed $\sqrt{s}$:

$$C_2^{ab}(M)=\rho_2^{ab}(M)-\rho_1^a\otimes\rho_1^b(M)\,. \tag{12}$$

In (12), ρ_2^{ab} is the familiar normalised two-particle invariant-mass spectrum. The second term describes the uncorrelated "background" and is at fixed mass of the pair given by:

$$\rho_1^a\otimes\rho_1^b(M)=\int\frac{\mathrm{d}^3p_1}{E_1}\int\frac{\mathrm{d}^3p_2}{E_2}\,\rho_1^a(q_1)\,\rho_1^b(q_2)\times\delta\{[(q_1+q_2)^2]^{1/2}-M\}\,, \tag{13}$$

with the normalisation:

$$\int\rho_1^a\otimes\rho_1^b\,dM=\langle n_a\rangle\langle n_b\rangle\,. \tag{14}$$

The integral over M of $C_2(M)$ in (12) is equal to the second-order integrated factorial cumulant or Mueller moment [11],

$$C_2^{ab}=\int C_2^{ab}(M)\,dM=\langle n_a(n_b-\delta_{ab})\rangle-\langle n_a\rangle\langle n_b\rangle\,. \tag{15}$$

In direct correspondence with normalised factorial moments and cumulants in intermittency analyses, we consider below the normalised functions

$$K_2^{ab}(M)=F_2^{ab}(M)-1\,, \tag{16}$$

with

$$F_2^{ab}(M)=\rho_2^{ab}(M)/\rho_1^a\otimes\rho_1^b(M)\,. \tag{17}$$

For three-particle systems, we define the "connected" correlation function (or factorial cumulant) in the usual way

$$\begin{aligned}C_3^{abc}(q_1,q_2,q_3)\equiv\rho_3^{abc}&-\rho_1^a(q_1)\,\rho_2^{bc}(q_2,q_3)\\&-\rho_1^b(q_2)\,\rho_2^{ca}(q_1,q_3)\\&-\rho_1^c(q_3)\,\rho_2^{ab}(q_1,q_2)\\&+2\,\rho_1^a(q_1)\,\rho_1^b(q_2)\,\rho_1^c(q_3)\,.\end{aligned} \tag{18}$$

Integration over all variables, except $M^2=(q_1+q_2+q_3)^2$ yields

$$C_3(M)\equiv\rho_3(M)-\{\rho_1^a\otimes\rho_2^{bc}(M)+\text{perm.}\}+2\,\rho_1^a\otimes\rho_1^b\otimes\rho_1^c(M)\,, \tag{19}$$

$$K_3(M)=C_3(M)/\rho_1^a\otimes\rho_1^b\otimes\rho_1^c(M)\,. \tag{20}$$

To calculate the background term (13) one may apply a Monte-Carlo method as in [7]. Here we use a "track-pool" or "event-mixing" technique, similar to that used in studes of Bose-Einstein (BE) correlations and in the "correlation-integral" method [12]. The procedure is as follows. A pool of particle four-vectors is constructed from a large number of events. Then, to build an "uncorrelated" event, track-multiplicities N_i for particles of type i are chosen according to a Poissonian with a fixed average, and N_i particles of the desired type are randomly selected with equal probability from the "pool", ensuring that each particle originates from a different event. The fake events then undergo the same treatment as the real events. The mass-spectra $\rho_2(M)$ and $\rho_1\otimes\rho_1(M)$ are normalised to their respective experimental values (7) and (14) in the studied kinemtatical region.

The same technique is easily generalised to three- or higher-order correlation functions. For example, a term $\rho_1^a\otimes\rho_2^{bc}(M)$ in (19) is calculated taking from each event one track of type (b) and type (c), and a third track of type (a) from another event.

Before describing the data, it is useful to elaborate somewhat on the physical meaning of (12) [7, 8]. For independently produced particles $C_2(M)$ is necessarily zero if kinematical constraints can be neglected. If par-

ticles are produced exclusively via the two-body decay of a resonance or cluster (hardly realistic for $\pi^{\pm}\pi^{\pm}$-pairs), then $C_2(M)$ measures directly the dynamical correlation within the cluster. Two particles originating from different resonances contribute only to the background (provided one may neglect interference effects). Not eliminated from C_2 are, therefore, those pairs which are the decay products of an m-particle resonance ($m \geqq 3$). The function C_3 has an analogous meaning.

3 Experimental results

3.1 Invariant-mass dependence of C_2

To illustrate the method and the general trend of the data, we show in Fig. 1 $\rho_2(M)$, $\rho_1 \otimes \rho_1(M)$ and $C_2(M)$ for $(--)$ and $(+-)$ charge-combinations in full phase space. The distributions $\rho_2(M)$ and $\rho_1 \otimes \rho_1(M)$ evidently extend to large M-values, but we shall be mainly interested in the region below 1 GeV.

One notices that $\rho_2(M)$ and $\rho_1 \otimes \rho_1(M)$ become equal, within errors, above a relatively small value of M. This gives confidence in the usefulness of the function $C_2(M)$ as a measure of dynamical correlation effects.

The function $C_2^{--}(M)$ is largest at threshold, slightly negative near $M \sim 0.8$ GeV and zero for $M > 1.5$ GeV; $\rho_2^{+-}(M)$, and $C_2^{+-}(M)$ in particular, reveal a clear ρ^0 signal. These functions are nearly zero for $M \geqq 1.5$ GeV.

Figure 2 compares in more detail C_2 for various charge combinations. Here, and for all following results, we limit the single particle c.m. rapidity to $|y| < 2$, unless specified otherwise. One observes that $C_2^{++}(M)$ and $C_2^{--}(M)$ practically coincide. In contrast, $C_2^{+-}(M)$ drops to zero at threshold; otherwise it is much larger, and has a very different shape compared to $C_2^{\pm\pm}$. Qualitatively, this is easily understood. Besides direct contributions from resonances in the $(+-)$-channel, additional correlations are generated by other states (such as η, η', ω, A_2,...) decaying into higher multiplicity channels. An anologous contribution, but much smaller in magnitude and concentrated at lower mass is expected for like-sign pairs. For these, in addition, interference effects due to Bose-Einstein symmetrisation of resonance- and prompt-particle production amplitudes will enhance the invariant-mass region close to threshold [8, 13].

For the second-order Mueller moment we obtain $C_2^{--} = 0.79 \pm 0.05\,(0.71 \pm 0.04)$, $C_2^{++} = 0.89 \pm 0.08\,(0.74 \pm 0.02)$, $C_2^{+-} = 3.65 \pm 0.07\,(2.68 \pm 0.05)$ for all M (for $M < 0.8$ GeV). Consequently, the region below 0.8 GeV in $C_2^{--}(M)$ or $C_2^{++}(M)$ accounts for $\sim 90\%$ of all correlations; for $C_2^{+-}(M)$ this is significantly smaller ($\sim 73\%$).

The behaviour of $C_2^{cc}(M)$ in Fig. 2 combines the features of the charge-separated states and is therefore less instructive*. Nevertheless, in many intermittency analyses charges are not distinguished. We shall, therefore, continue to present (cc)-data in the rest of the paper.

It is instructive to compare the results presented in Fig. 2 with our previous study of C_2 in rapidity space. In

* Note that $C_2^{cc} \equiv C_2^{++} + C_2^{--} + 2\,C_2^{+-}$

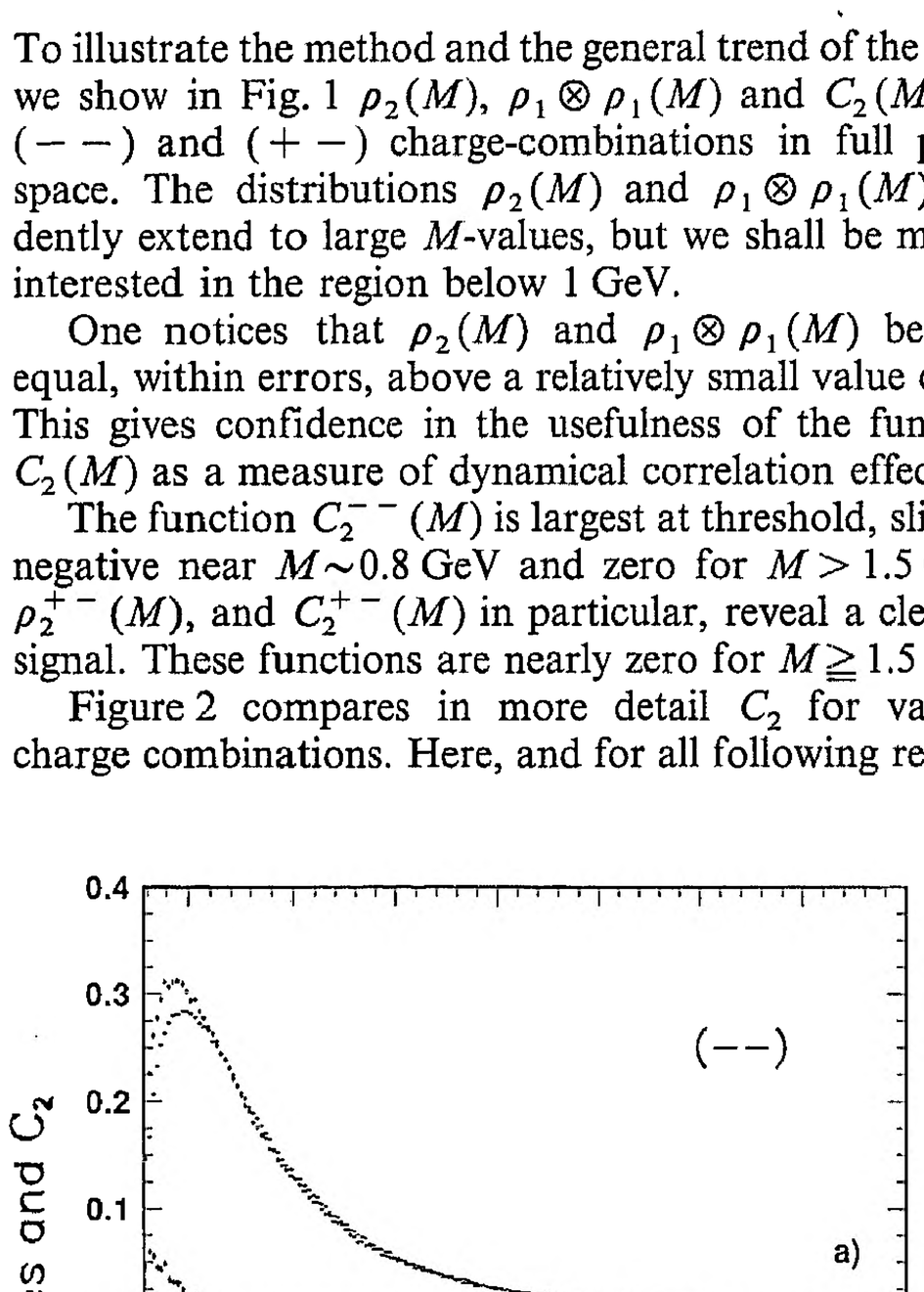

Fig. 1a, b. The densities $\rho_2(M)$ (upper), $\rho_1 \otimes \rho_1(M)$ (middle) and the correlation function $C_2(M)$ (lower) for $(--)$- and $(+-)$-pairs produced in $\pi^+ p$ and $K^+ p$ interactions (combined) in full phase space

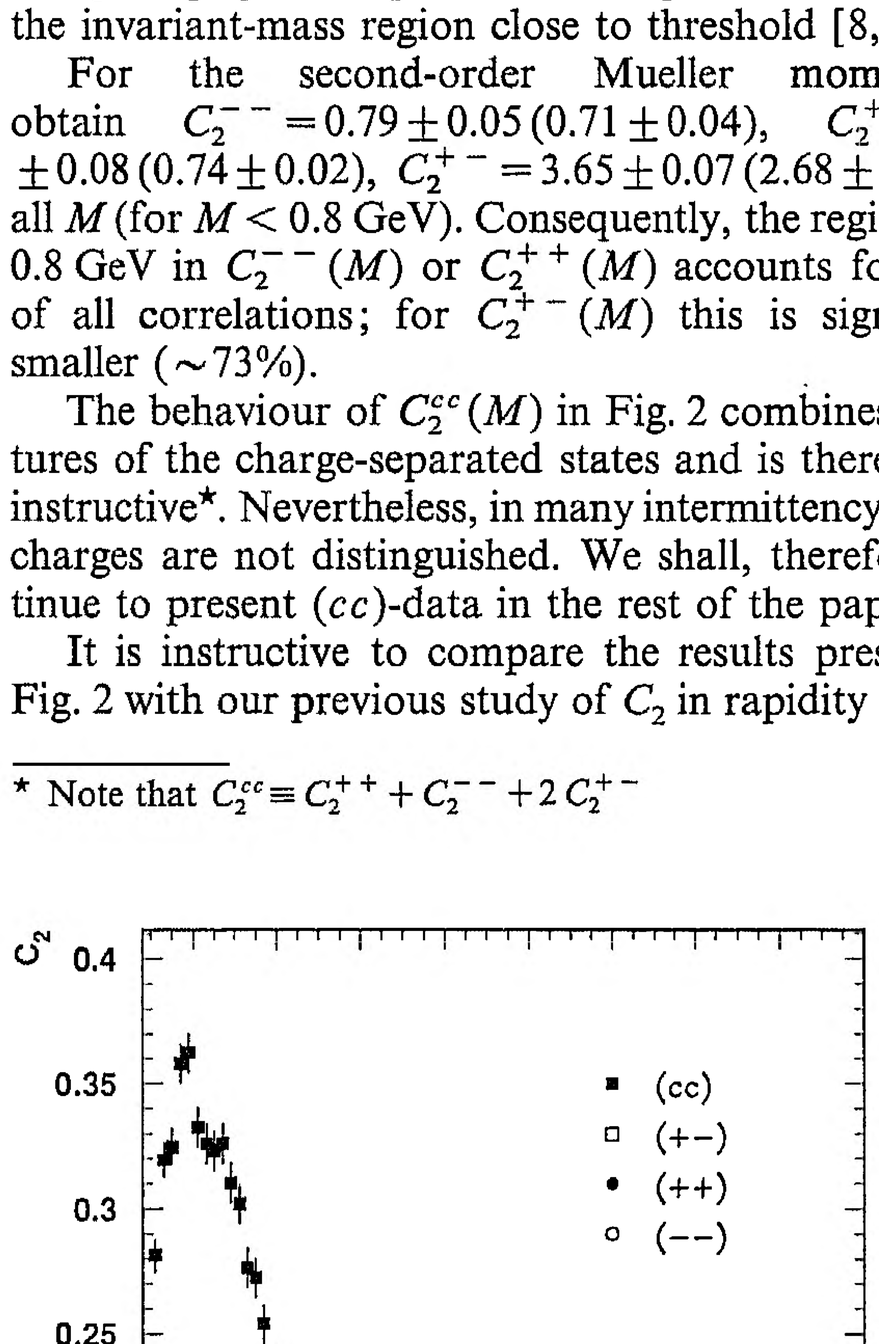

Fig. 2. The correlation function $C_2(M)$ for the indicated charge combinations for particles with c.m. rapidity $|y_i| < 2$ $(i = 1, 2)$

[14] we found that the correlation functions $C_2(y_1, y_2)$ for different charge-states, while differing in absolute values near $y_1 = 0$, all have a similar Gaussian shape with a dispersion ranging from ~ 0.8 for $(--)$-pairs to ~ 1 for $(+-)$-pairs. Figure 2 illustrates that the similarity in rapidity space is superficial and hides the true nature of the dynamical correlations. The correlation functions for like- and unlike-sign pairs indeed differ strongly when studied in terms of invariant mass, for the reasons mentioned earlier in this section.

3.2 Normalised second-order factorial cumulants

Intermittency studies deal with normalised factorial moments and factorial cumulants in small domains of phase space. We, therefore, turn to a presentation of the data on the normalised cumulant function $K_2(M)$.

Figure 3 shows $K_2^{+-}(M)$, $K_2^{cc}(M)$, $K_2^{--}(M)$ and $K_2^{++}(M)$ for particles with rapidity $|y| < 2$ (open symbols) and $|y| < 0.5$ (solid symbols). These figures demonstrate that also $K_2(M)$ is very different for like- and unlike-charge pairs.

For like-charge pairs, K_2 drops in a power-like manner and is close to zero for masses around 1 GeV. Unlike-charge pairs show a clear ρ^0 contribution in particular for $|y| < 0.5$. Otherwise, the correlation function has a much weaker M-dependence than like-charge pairs. For all charge combinations, the correlation is stronger for $|y| < 0.5$ than for $|y| < 2$.

The lines in Fig. 3 are fits by a power-law

$$K_2(M) = A(1/M^2)^{\beta}. \tag{21}$$

The best-fit parameters are collected in the first four lines of Table 1. Lines 5 and 12 (see further) are results of a fit using invariant-mass bins of 4 MeV.

Figure 4, where the ratio $K_2^{--}(M)/K_2^{+-}(M)$ is plotted (for $|y| < 2$) offers a further illustration of the different M-dependence of the like- and unlike-charge correlation function. The curve represents the function (21)

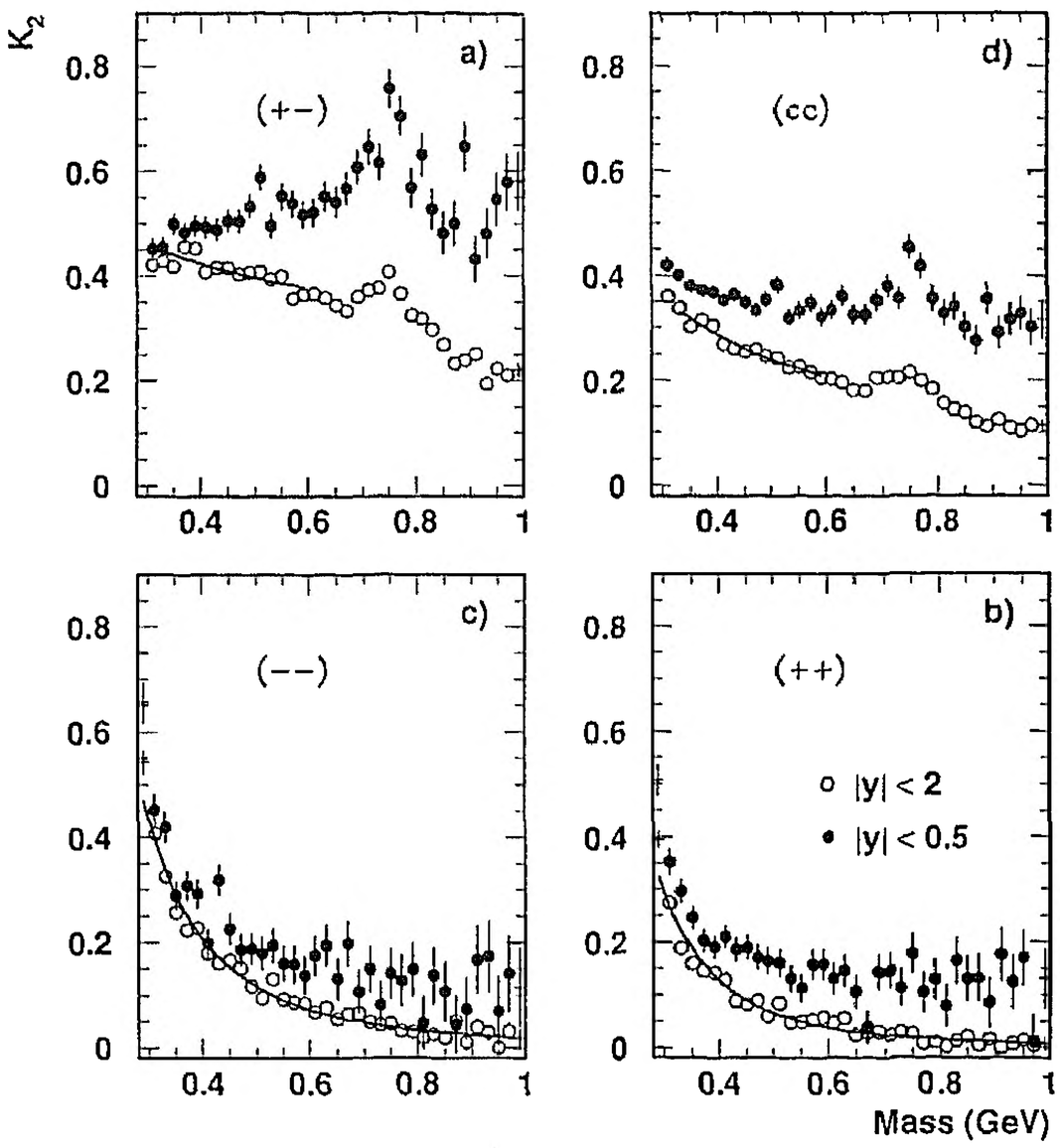

Fig. 3a–d. The normalised second-order factorial cumulant versus invariant mass for particles with c.m. rapidity $|y_i| < 2$ and $|y_i| < 0.5$, respectively. Lines are fits by $A(1/M^2)^{\beta}$ (see Table 1)

with $\beta = 1.02 \pm 0.06$, fitted in the range $0.32 < M < 0.8$ GeV. The value of β is consistent with unity, a value often quoted for the difference in Regge-intercept of an "exotic" and "standard" (ρ, f) trajectory [7]. We shall not further elaborate on a possible Mueller-Regge interpreation (see [7]) which is considered to be doubtful at small M, but merely note that i) the Dual Mueller-Regge approach, with factorisation, leads in a natural way to power-law dependence in invariant mass of the correlation functions, ii) the data in [7], and those presented here, are not in contradiction with this picture.

Table 1. Fits with the form $A(1/M^2)^{\beta}$ to the second- and third-order factorial cumulant $K_2(M)$ and $K_3(M)$ in M^+p interactions at 250 GeV/c incident beam momentum, in indicated invariant-mass intervals and for various cuts (p_T in GeV/c).

K_2, K_3	M(GeV)	Cut	A	β	χ^2/NDF
cc	0.30–0.6	–	0.136 ± 0.004	0.41 ± 0.02	20/13
$+-$	0.30–0.6	–	0.315 ± 0.010	0.17 ± 0.02	30/11
$++$	0.34–1.0	–	0.011 ± 0.001	1.30 ± 0.07	25/31
$--$	0.34–1.0	–	0.024 ± 0.001	1.15 ± 0.05	32/31
$--$	0.28–1.0	–	0.019 ± 0.002	1.29 ± 0.04	226/178
$--$	0.28–0.6	$\Phi < 45°$	0.014 ± 0.001	2.45 ± 0.24	60/34
$--$	0.28–1.0	$45° < \Phi < 135°$	0.022 ± 0.002	1.32 ± 0.05	42/34
$+-$	0.34–1.0	$\Phi < 45°$	0.080 ± 0.006	0.72 ± 0.05	23/15
$+-$	0.34–1.0	$45° < \Phi < 135°$	0.26 ± 0.01	0.35 ± 0.02	31/15
$--$	0.28–1.0	$p_T < 0.15$	0.013 ± 0.001	1.54 ± 0.24	41/34
$--$	0.28–1.0	$0.15 < p_T < 0.3$	0.022 ± 0.004	1.36 ± 0.08	43/34
$--$	0.28–1.0	$p_T > 0.15$	0.015 ± 0.002	1.35 ± 0.07	202/178
$---$	0.42–1.0	–	0.005 ± 0.002	3.37 ± 0.32	41/26
$+++$	0.42–1.0	–	0.015 ± 0.007	3.84 ± 0.99	28/26
$++-$	0.42–1.0	–	0.085 ± 0.004	1.16 ± 0.06	10/26
$--+$	0.42–0.8	–	0.12 ± 0.02	1.0 ± 0.1	11/15
$\frac{--}{+-}$	0.32–0.8	–	0.07 ± 0.01	1.02 ± 0.06	25/22

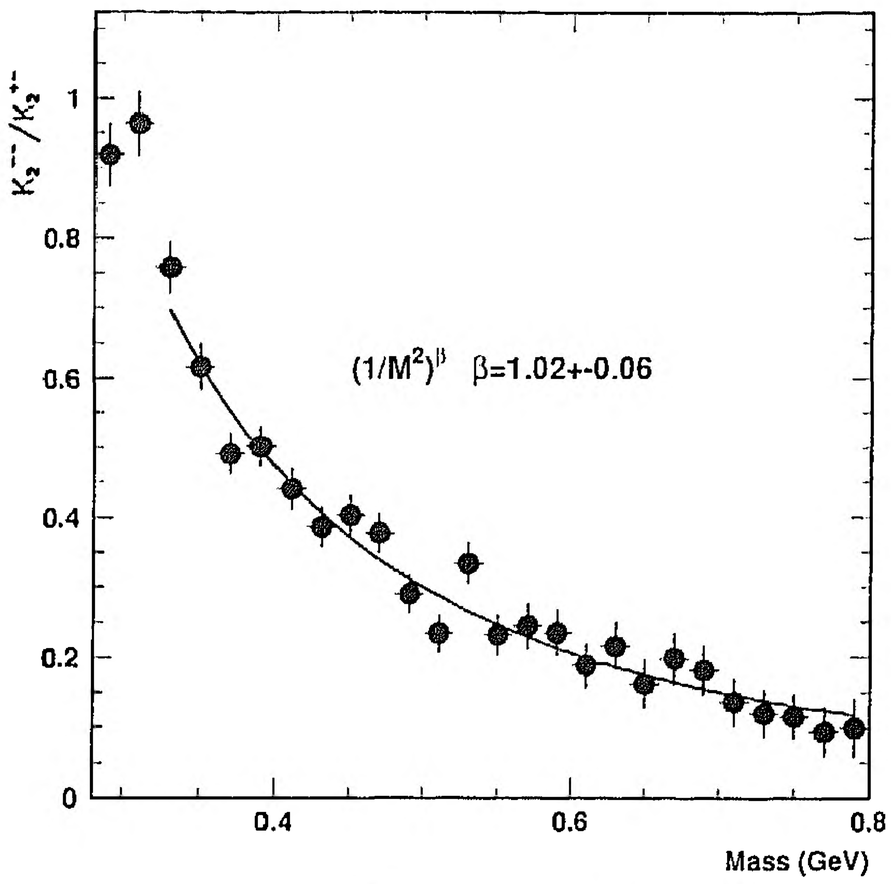

Fig. 4. The ratio of $K_2^{--}(M)$ and $K_2^{+-}(M)$ fitted by $A(1/M^2)^\beta$ (for $|y_i| < 2$)

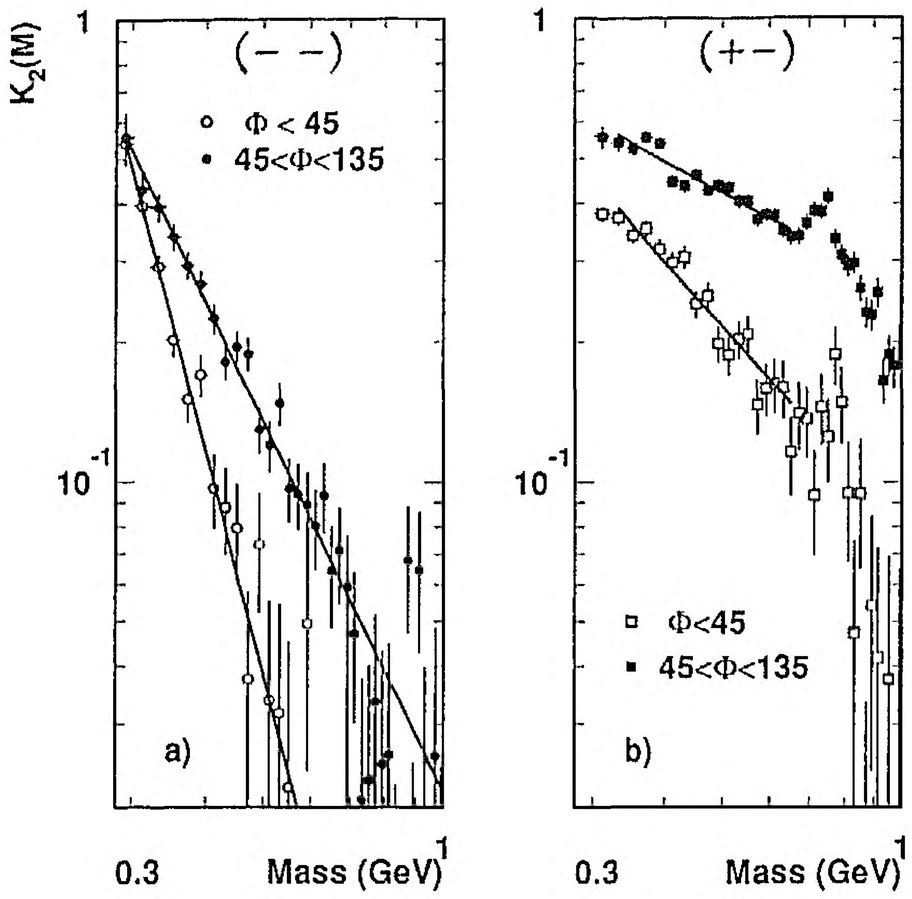

Fig. 6a, b. Normalised second-order factorial cumulants in intervals of relative azimuthal angle Φ. Lines are fits by $A(1/M^2)^\beta$ (see Table 1)

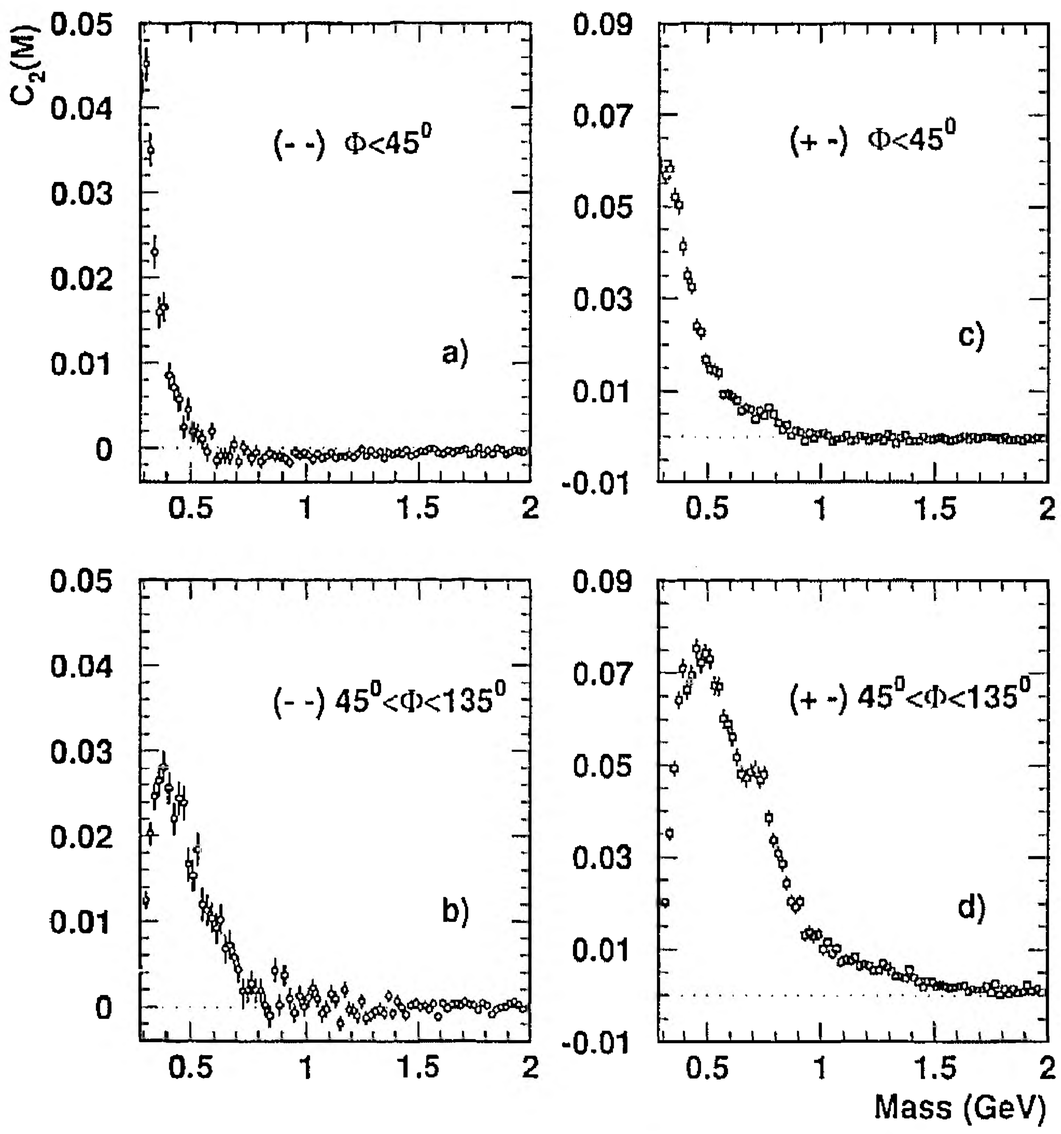

Fig. 5a–d. The correlation function $C_2^{--}(M)$ and $C_2^{+-}(M)$ in intervals of relative azimuthal angle Φ (in degrees)

The features shown by Fig. 5 are partly kinematical since small relative angles between the particle momenta favour small invariant mass. This kinematical effect equally affects $\rho_1 \otimes \rho_1(M)$. Dynamics is, therefore, better seen in $K_2(M, \Phi)$, displayed in Fig. 6 in a double-log scale. This function has the strongest M-dependence for $\Phi < 45°$. With this cut, also the ρ^0-signal is considerably reduced in $(+-)$-pairs. The lines are fits by (21) with parameters given in lines 6 and 7 of Table 1. We note, in particular, that $K_2^{--}(M)$ is power-behaved from threshold up to ~ 1 GeV.

Figure 7a shows in more detail the dependence of K_2 on azimuthal angle for masses close to threshold, $M < 0.4$ GeV. $K_2^{--}(M)$ is nearly constant apart from some depletion in the interval $0 < \Phi < 30°$; $K_2^{+-}(M)$ rises gently to reach a nearly constant value for $\Phi > 80°$. The Φ-dependence is more pronounced in the interval $0.5 < M < 1$ GeV (Fig. 7b), in particular for $(+-)$-pairs.

From the data presented in this section, we conclude that the p_T-integrated normalised correlation function depends weakly on the azimuthal separation of the pair in the small-mass region, especially for like-charge combinations: the correlation function depends mainly on invariant mass. Both $K_2^{--}(M)$ and $K_2^{+-}(M)$ are power-behaved, the latter for $M < 0.6$ GeV.

3.3 Azimuthal angle dependence

In Fig. 5 we plot $C_2^{--}(M, \Phi)$ and $C_2^{+-}(M, \Phi)$ in various intervals of Φ, the angle between the transverse momenta of the pair.

Both for $(+-)$ and $(--)$ we observe a strong positive correlation at small M and small Φ, substantially narrower for $(--)$-pairs than for $(+-)$-pairs. The ρ^0 signal stands out more clearly for $45° < \Phi < 135°$ than in the other distribution.

3.4 Transverse momentum dependence

The observation by NA22 [15] that the intermittency effect is most pronounced for low-p_T particles (e.g. $p_T < 0.15$ GeV/c) and almost absent for larger p_T-values, has attracted much attention since it pointed to intermittency in hadron-hadron collisions as a "soft" effect. Low-p_T intermittency is also visible in the UA1 data [16] in spite of the bias against small p_T in this experiment. The reason for stronger intermittency remained rather

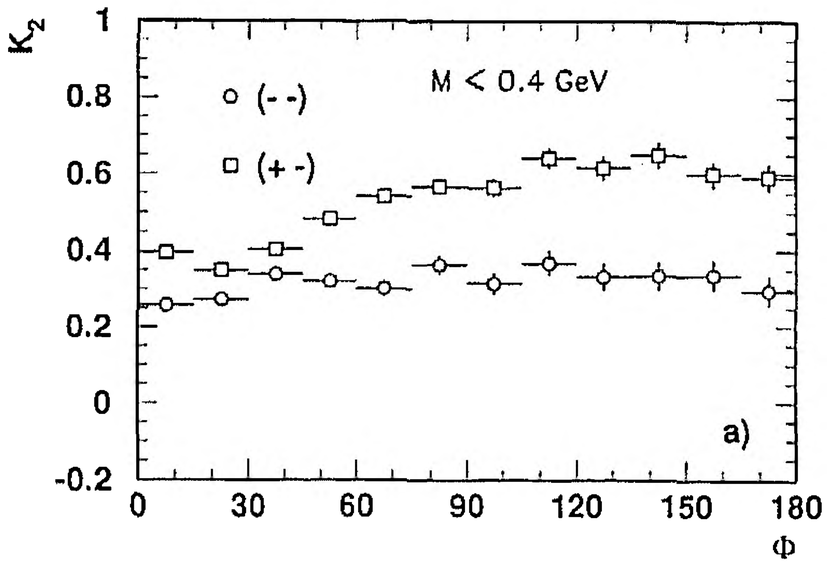

Fig. 7a, b. Normalised second-order factorial cumulants versus relative azimuthal angle for invariant masses **a** $M < 0.4$ GeV, **b** $0.5 < M < 1$ GeV

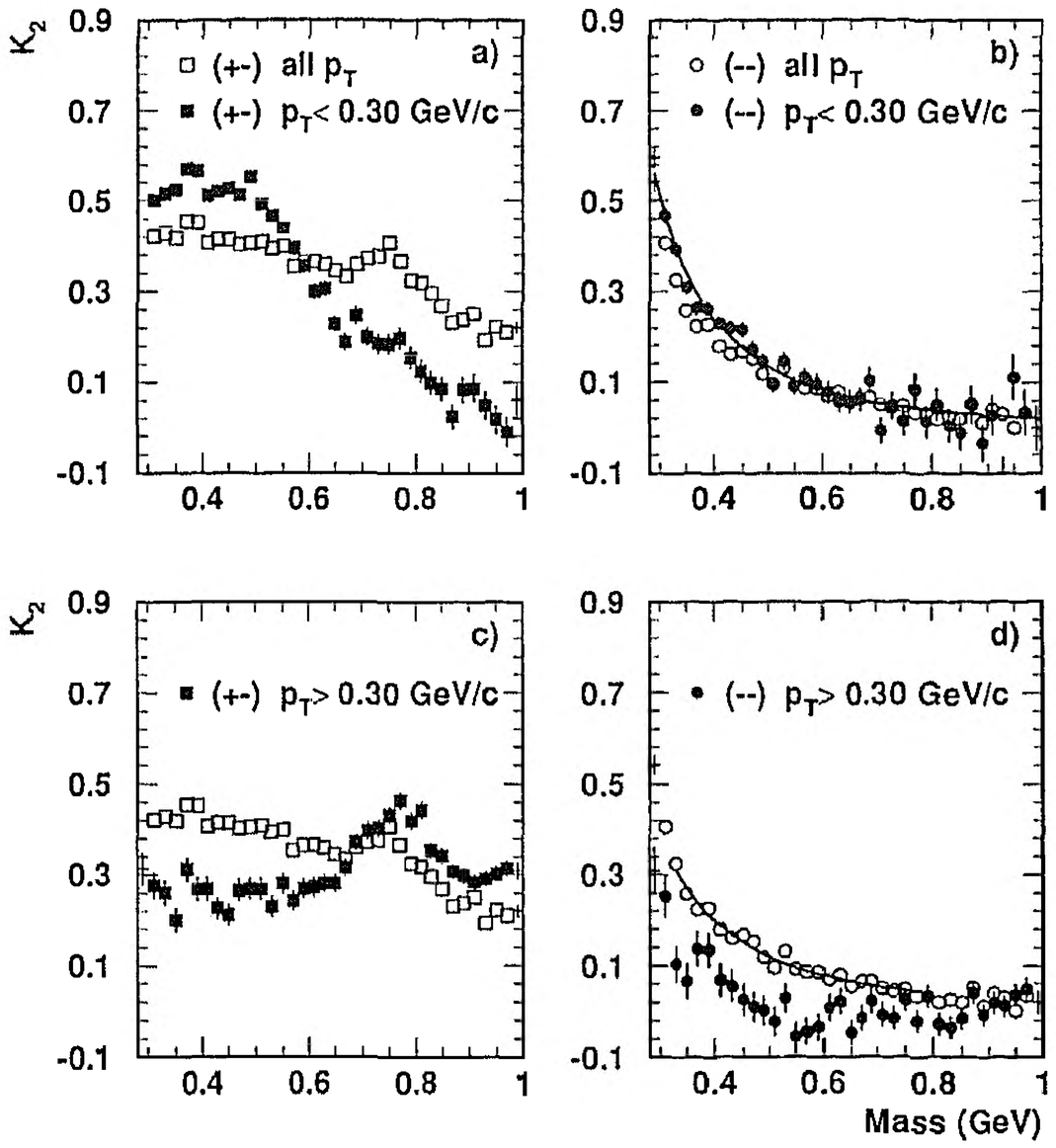

Fig. 9a–d. The normalised second-order factorial cumulants with restricted transverse momentum of the individual particles. Lines are fits by $A(1/M^2)^{\beta}$ (see Table 1)

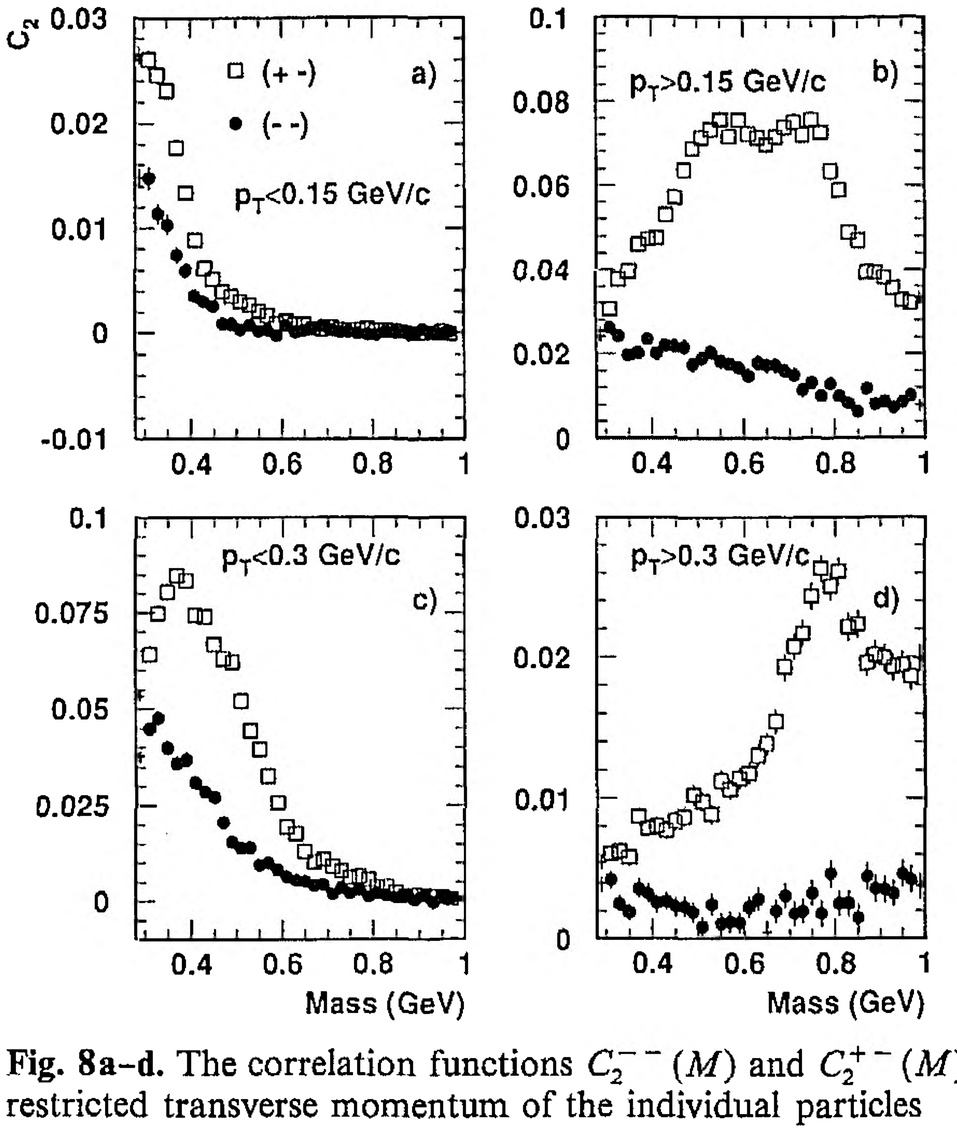

Fig. 8a–d. The correlation functions $C_2^{--}(M)$ and $C_2^{+-}(M)$ with restricted transverse momentum of the individual particles

unclear and, moreover, the effect could not be reproduced by presently used models.

To try and clarify this issue, we here study $C_2(M)$ and $K_2(M)$ in different intervals of transverse momentum. Figure 8 shows $C_2^{+-}(M)$ and $C_2^{--}(M)$ for particles with transverse momentum below and above 0.15 and 0.30 GeV/c, respectively.

For low-p_T particles (Fig. 8a, c), C_2 drops more rapidly to zero with increasing M than the all-p_T data (Fig. 2); $C_2^{--}(M)$ is zero, within errors, above 0.5 GeV. For $C_2^{+-}(M)$ this happens for $M \sim 0.7$–0.8 GeV. Note also that the otherwise prominent ρ^0-signal is nearly completely removed by the p_T-cut.

Imposing a lower limit on p_T (Figs. 8b, d) has the effect of enhancing the correlation at larger M and increases the influence of the ρ^0-meson. For $p_T > 0.3$ GeV/c, C_2^{--} is close to zero in the whole mass range studied ($M \leqq 1$ GeV).

As already hinted in Sect. 2.2, cuts on transverse momentum strongly influence the mass-spectra and C_2 for (trivial) kinematical reasons. Since this affects $\rho_2(M)$ and $\rho_1 \otimes \rho_1(M)$ alike, it is more instructive to consider the functions K_2. Examples of these are shown in Figs. 9a–d for $(+-)$- and $(--)$-pairs. For ease of comparison we also include the data for all p_T.

For $K_2^{+-}(M)$ (Fig. 9a), the selection $p_T < 0.3$ GeV/c eliminates most of the ρ^0-contribution; K_2 now has a much stronger dependence on M, compared to the all-p_T data. A likely explanation is that reflections from e.g. three-body resonance decays in the $(+-)$-channel are enhanced by the small-p_T cut. With $p_T > 0.3$ GeV/c (Fig. 9c), the ρ^0 stands out most prominently; the correlation function shows little M-dependence for $M < 0.6$ GeV.

From Fig. 9b, we note the interesting feature that $K_2^{--}(M)$ is hardly affected by the cut. This is also true for $p_T < 0.15$ GeV (not shown). For example, from a fit by the form (21) we find $\beta^{--} = 1.54 \pm 0.24$ and $\beta^{--} = 1.35 \pm 0.07$ for $p_T < 0.15$ GeV/c and

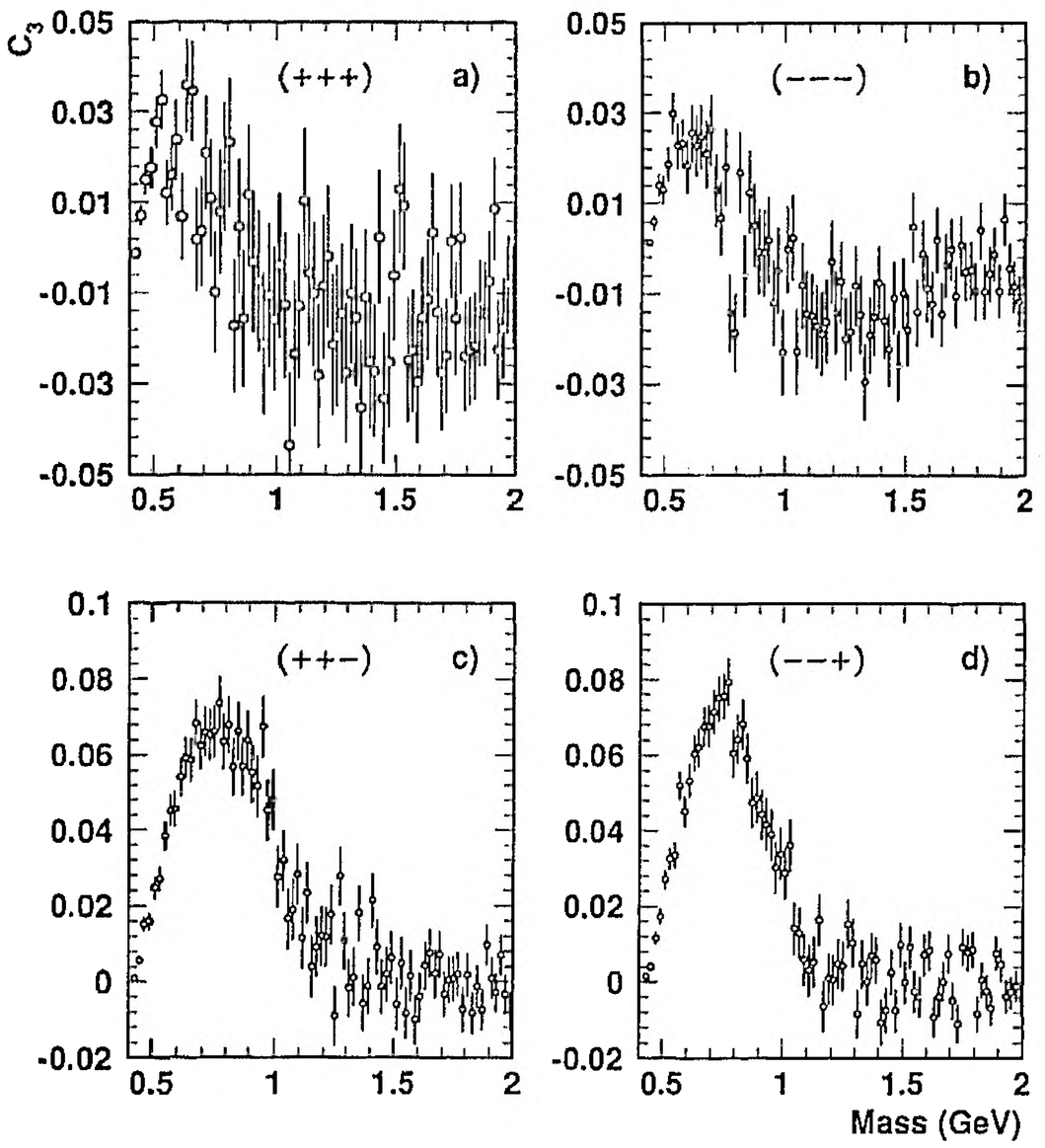

Fig. 10a–d. The third-order correlation function $C_3(M)$ for various charge combinations

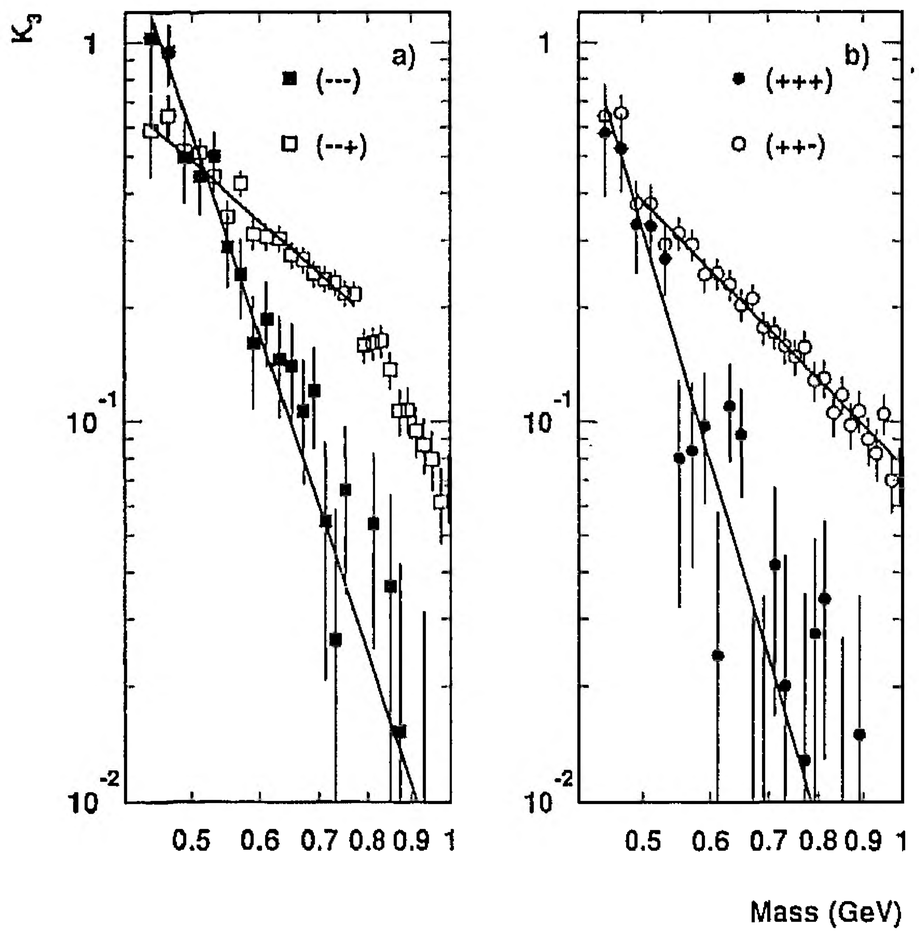

Fig. 11a, b. The third-order normalised factorial cumulant $K_3(M)$ for various charge combinations. Lines are fits by $A(1/M^2)^{\beta}$ (see Table 1)

$p_T > 0.15$ GeV/c, respectively, to be compared with $\beta^{--} = 1.29 \pm 0.04$ for all p_T (cf. Table 1). For $p_T > 0.3$ GeV/c, $K_2^{--}(M)$ is reduced in value for kinematical reasons.

We conclude that the two-particle correlation function of $(--)$-pairs* – a priori a function of five variables at fixed $\sqrt{s}$ – shows the strongest explicit dependence when studied in terms of the invariant-mass variable, at least in the small-mass region where intermittency is searched for.

The correlation function of unlike-charge pairs is influenced by direct-channel resonances and resonance reflections and is a more complicated function of the kinematical variables.

3.5 Three-particle cumulants

In Fig. 10 we present C_3, the third-order correlation function, as a function of the three-particle invariant mass. Non-exotic triples show a strong correlation below $M < 1.2$ GeV. For identical-particle triplets, errors are large, but a positive correlation is clearly seen for masses below 1 GeV.

The normalised cumulants K_3 are displayed in Fig. 11. The lines are power-law fits of the form (21) to the data with parameters given in Table 1. The $(---)$-triplet data (Fig. 11a) exhibit an unexplained shoulder near 0.8 GeV, not seen in the charge-conjugate triplet (Fig. 11b). Nevertheless, cumulants of non-exotic triplets decrease as a power in $1/M^2$ with a slope $\beta \sim 1.0$–1.2, considerably faster than $(+-)$-pairs. Identical-particle triplets fall even steeper with M, with slopes of the order of 3.

4 Comparison to FRITIOF

The experimental study of factorial moments as a function of cell-size has revealed serious shortcomings in the Monte-Carlo generators commonly used to simulate multiparticle production processes. Discrepancies are largest between models* and data for hadron-hadron (and hA or AA) processes. For e^+e^- annihilations the generators based on JETSET [19–21] (or HERWIG [22, 23]) are much more successful. The reason why models which use essentially the same hadronisation algorithm (JETSET) for e^+e^- annihilation as for hh processes, fare so differently, still remains obscure.

In a previous study of rapidity correlations [24], serious disagreements of FRITIOF (and other models) with the data were reported. We have already mentioned that rapidity correlations are very insensitive to dynamical effects at small invariant mass and it is, therefore, not too surprising that the cause of the model failures remained unclear. In this section we show that analysis of correlations in terms of invariant mass not only confirms that FRITIOF – or rather JETSET – fails, but the method reveals specific deficiencies that need to be remedied. As will become clear, these are apparently not so much related to "new physics" but rather to a number of defects which have passed unnoticed.

We use FRITIOF, version 2, with parameter settings as described e.g. in [25]. We opt for this version – although more recent versions are now available – since it has been used in studies of many other topics in this

* This also holds for $(++)$-pairs not discussed here

* Here we consider the specific example of FRITIOF [17] but the same is true for e.g. the two-string dual parton model [18]

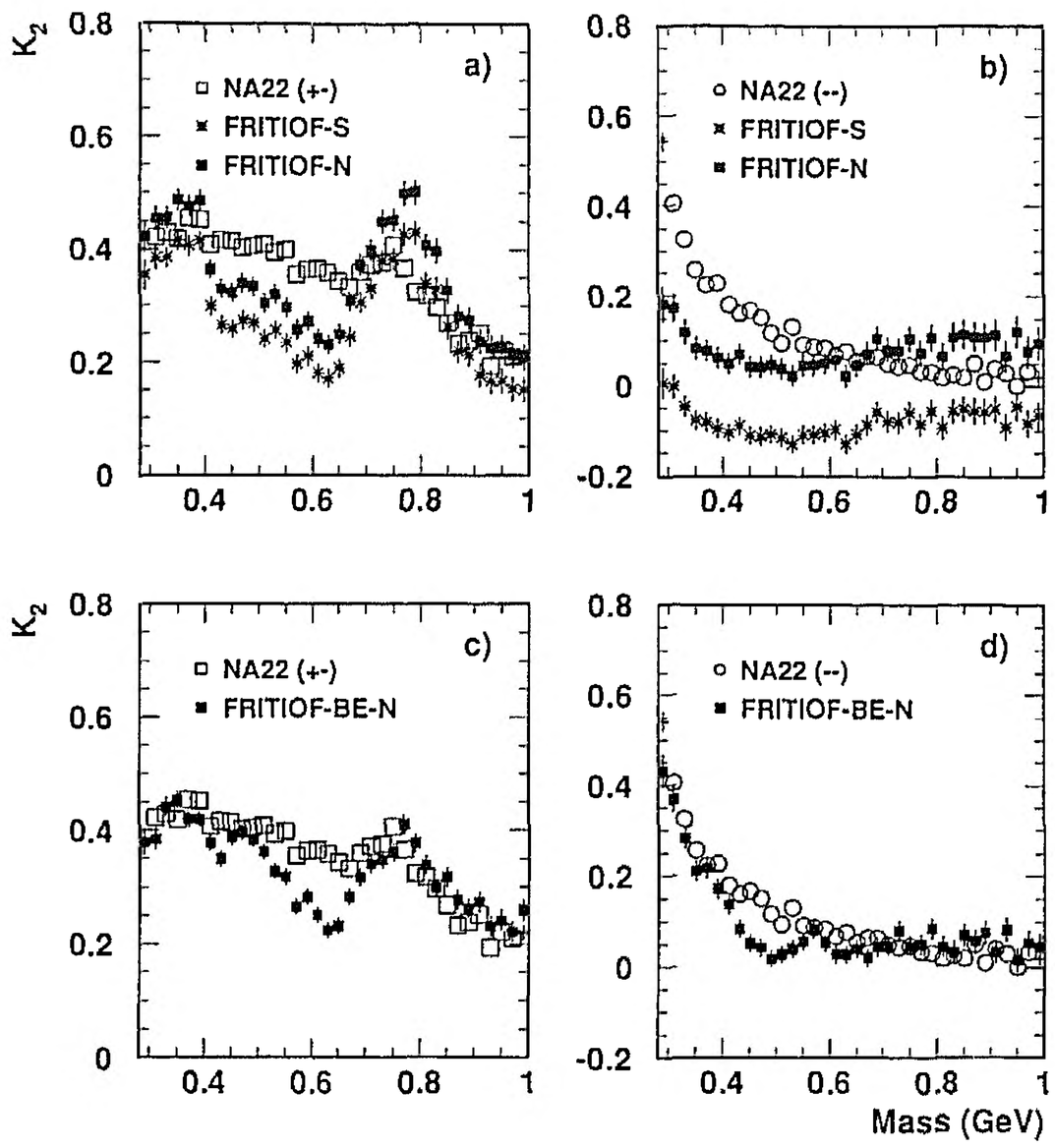

Fig. 12a–d. The normalised second-order factorial cumulant $K_2^{+-}(M)$ and $K_2^{--}(M)$ compared to FRITIOF 2. Predictions in **a–b** for FRITIOF and JETSET 6.3 with default parameters (FRITIOF-S) and renormalised (FRITIOF-N); **c–d** for FRITIOF rescaled, with Bose-Einstein enhancement and suppressed resonance production rates in JETSET

experiment. Since we are ultimately interested in a better understanding of the behaviour of factorial moment data, we limit the discussion to normalised factorial cumulants.

Figure 12a–b compares the data on $K_2^{+-}(M)$ and $K_2^{--}(M)$ to FRITIOF-S, the standard FRITIOF version with default NA22 parameters. The prediction for $K_2^{+-}(M)$ (Fig. 12a) bears little resemblance to the data: i) the predicted ρ^0-signal is too strong, ii) the correlation function falls much faster with M in the region below $M < 0.6$ GeV.

It is known that FRITIOF underestimates the width of the full phase-space (charged particle) multiplicity distribution or, equivalently, the second-order factorial cumulant, integrated over all M. To remove this global defect, we renormalized the FRITIOF predictions to the experimental values of K_2^{--} and K_2^{+-} for all M. The corresponding results are indicated as FRITIOF-N in Fig. 12. As to the structure in the region below $M = 0.6$ GeV, we find from FRITIOF that is due to reflections from η, η' and ω decays.

From previous NA22 studies, it is known that JETSET, with default parameters, overestimates the η production rate [25, 26] by as much as a factor of three. There are also indications from this and other experiments that the inclusive cross section of ρ^0 [27–30] and η' [31] is too large in JETSET by a similarly large factor. The influence on correlation functions and factorial moments of such deficiencies in the Monte Carlo's was not fully appreciated in earlier intermittency studies, with the exception of [32].

Figure 12b compares FRITIOF to $K_2^{--}(M)$ data. The predicted correlation (small and slightly negative in FRITIOF-S) is roughly constant in M, except for a peak at threshold which is related to η' decays. Unfortunately, the inclusive η' cross section is not directly measurable in this experiment. It is, therefore, impossible to assess the importance of its contribution to the strong rise of $K_2^{--}(M)$ seen in the data for M approaching the threshold. Still, if we assume that the η'-rate is overestimated by roughly the same amount as the η-rate, it becomes clear that another dynamical effect, present in the data but not in FRITIOF or JETSET, is responsible for the sharp decrease of $K_2^{--}(M)$ from threshold to $M \sim 0.6$ GeV.

A low-mass enhancement of the type seen in Fig. 12b is, of course, expected from Bose-Einstein interference. By this we mean small-mass enhancements which are the consequence of symmetrisation of production amplitudes. These include interferences between "prompt" production amplitudes, as well as those between "prompt"- and resonant final-state interactions. The net effect of all these is obviously difficult to estimate without a detailed model calculation at the amplitude level. Simplified treatments can be found in [13, 8] (see also [33]). In general such calculations predict strong enhancements of the correlation function at very small masses. Under the (extremely naive) assumption that pions are emitted from a production volume with an extension of the order of the pion Compton wavelength (1.4 fm) without suffering any interaction – hardly likely in a strong interaction process – one would expect to observe a Bose-Einstein effect from threshold up to about 0.4–0.5 GeV.

To assess the importance of (naive) Bose-Einstein correlations, we have incorporated in FRITIOF such an enhancement, using the algorithm developed by Sjöstrand for JETSET 7.3 [34, 35]. We use an exponential parametrisation in $|Q|$:

$$\mathrm{BE}(M) = 1 + \lambda e^{-R|Q|}, \tag{22}$$

with $\lambda = 0.5$ and $R = 0.8$ fm.

Furthermore, to appreciate the influence of pseudoscalar and vector mesons, we have introduced ad hoc modifications* in JETSET which reduce the ρ^0 (η and η') production rate to 1/2 (1/3) of the "default" rate.

The results, indicated as FRITIOF-BE-N, are shown in Figs. 12c, d. For $K_2^{+-}(M)$, agreement is acceptable in and above the ρ^0-region and below $M < 0.5$ GeV, but not in the intermediate mass region. For $K_2^{--}(M)$, FRITIOF agrees with the data (after global renormalisation, see before) for $M > 0.6$ GeV. Nevertheless, the M-dependence remains too strong in the region around 0.5 GeV.

We should stress that the value of λ, which determines the strength of the BE-effect, is rendered quite uncertain by the unknown contribution from η', as discussed earlier. With this caveat, we are tempted to conclude that a

* One should note that such a "brute-force" procedure is hardly acceptable in the framework of the LUND fragmentation picture and is likely to adversely affect agreement with other observables which are otherwise well described

BE-effect of a "traditional" form (22) could explain the enhancement of $K_2^{--}(M)$ for $M \leqq 0.4$ but the remaining deviations require further study.

For three-particle correlations, the FRITIOF predictions for $C_3(M)$ (not shown) are close to zero for all values of M, contrary to the data.

In summary, we learn from the FRITIOF calculations that the model's difficulties in reproducing the measured correlation functions are to a large extent caused by i) incorrect production rates of (at least) ρ^0, η, and, possibly ω and η' mesons, ii) the absence of a Bose-Einstein small-mass enhancement mechanism.

Whether there is evidence for "new physics" in the data is difficult to judge at present. It remains to be seen if the most obvious deficiencies in particle and resonance production rates can be cured in a consistent manner in models such as JETSET. The apparent success of the Parton-Shower + JETSET Monte-Carlo in e^+e^- annihilations most likely means that correlations are less sensitive to resonance and Bose-Einstein effects at LEP energies or, that the model parameters are tuned to the data in a way which compensates for the deficiencies.

5 Discussion and conclusions

In this paper we have studied two- and three-particle correlations in various charge combinations in terms of the invariant mass of pairs and triplets. This work was motivated by the recently revived interest in correlation phenomena, and, in particular, the considerable experimental and theoretical effort invested in the search for intermittency and fractal dynamics.

The work on intermittency initially concentrated on the behaviour of factorial moments of the charged multiplicity distribution in progressively decreasing intervals of rapidity. This geometric "box-counting" approach, familiar in fractal theory, was soon extended to two- and three-dimensional phase space. Due to the highly non-uniform particle population, such analyses necessitated the use of variable transformations [36, 37] which considerably complicated interpretation of the results in terms of known dynamical effects and experimental bias.

With the "correlation integral" technique [12], the emphasis returned to correlation measurements in terms of suitably defined inter-particle distances. This avoided the arbitrariness in the choice of geometrical volume and its subdivisions, inherent to the previous analysis methods. In present applications [38, 39], Lorentz-invariant distance measures such as Q^2 have proven to be most revealing. It is worthwhile to stress that cumulative, rather than differential quantities are studied with this technique, again inspired by fractal theory.

In this paper, we analysed differential distributions. The (apparent) loss in statistical accuracy, compared to cumulative quantities, is amply compensated by greater sensitivity to fine-structure.

The data presented here help in clarifying several aspects of earlier factorial moment analyses.

- The factorial cumulants $K_2(M)$ and $K_3(M)$ behave as powers in $(1/M^2)$ from threshold to ~ 1 GeV in invariant mass. This confirms earlier speculations [40, 6] that normalised correlation functions, rather than inclusive densities might show scale-invariance.
- Factorial cumulants of "exotic" particle combinations show the strongest dependence on invariant mass. For "non-exotic" combinations, such as $(+-)$-pairs, the M-dependence is much weaker. Moreover, it is sensitive to the kinematical region examined and clearly related to resonances occurring in this channel.
- "All-charged" data mix very different dynamics and should be interpreted with caution.
- For small masses, the function $K_2^{\pm\pm}$, depends weakly on the transverse momentum of the particles and on their relative azimuthal angle, and is mainly a function of invariant mass. This fact explains [41] why selection of low-p_T particles gives rise to *enhanced* intermittency in rapidity-space [15] but *weaker* intermittency in terms of correlation integrals [38], two, at first sight, contradictory conclusions.
- The much larger powers β for like-sign than for unlike-sign pairs and triplets mean that the intermittency effect is predominantly due to the former. Bose-Einstein type correlations are a natural candiate to explain this difference. Accepting this hypothesis, we conclude from our data that the BE-effect leads to normalised correlation functions which are power-behaved in $(1/M^2)$. This is at variance with the traditionally adopted parametrisation of the two-particle *density* in terms of Gaussians or exponentials in Q^2 with parameters related to interaction-volume dimensions and wavefunction coherence. However, it is easy to verify that a function of the type (22), expressed in terms of invariant mass is, with present accuracy, almost indistinguishable from a function of the form $1 + A(1/M^2)^\beta$ as suggested by the power law (21). As a result, and depending on the point of view taken, present BE-data can be used either as evidence for scale-invariance of K_2 in the invariant mass variable, or as a confirmation of the traditional BE-interpretation.
- The origin of the failures exhibited by models such as FRITIOF, is most clearly revealed in our analysis. These failures are not necessarily due to "novel" dynamics, absent (by definition) in the models. They are in first instance a consequence of a variety of defects – such as incorrect resonance production rates and absence of identical particle symmetrisation – which belong to "standard" hadronisation phenomenology. Still, these defects are not easy to cure in a consistent manner by simple parameter-tuning and "new" physics may be needed to restore internal consistency in e.g. string-fragmentation models of the LUND type. Indeed, present work [42] on this subject starts to provide hints that a purely probabilistic treatment of the break-up of colour fields might have to be supplemented with new mechanisms, somehow related to the chiral structure of the non-perturbative QCD vacuum.
- Originating mainly from the low invariant-mass region (typically < 1.5 GeV), it is not impossible that the observed correlations, being dominated by strong final-state interactions, are quite independent of the process

initiating the primary colour separation in the collision. This would explain "universality" in the sense discussed earlier.

● Many authors argue that "intermittency" is somehow connected to (nearly scale-invariant) perturbative QCD-cascading. Others strongly contest this view on the argument that QCD cascades have a limited extent even at LEP energies and are dominated by a very small number of "hard" emissions. In the former case, one may expect significant differences in the correlation functions at low mass for e^+e^-, on the one hand, and for hh, hA and AA collisions, on the other hand. Whatever the final outcome, if differences are found, they should be used to clarify the respective roles of perturbative and hadronisation phases in the different types of collision processes.

Acknowledgements. It is a pleasure to thank the EHS coordinator L. Montanet and the operating crews and staffs of EHS, SPS and H2 beam, as well as the scanning and processing teams of our laboratories for their invaluable help with this experiment. We are grateful to III. Physikalisches Institut B, RWTH Aachen, Germany, DESY-Institut für Hochenergiephysik, Zeuthen, Germany, Department of High Energy Physics, Helsinki University, Finland for early contributions to this experiment. We thank the Nederlandse Organisatie voor Wetenschappelijk Onderzoek (NWO) for support of this project within the program for subsistence to the former Soviet Union (07-13-038).

References

1. W.A. Zajc: Proc. Int. Workshop on Correlations and Multiparticle Production, Marburg, p. 439, M. Plümer, S. Raha, R.M. Weiner (eds.). Singapore: World Scientific 1991
2. St. Macellini: Proc. Joint Int. Lepton-Photon Symp. and Europhys. Conf. on High Energy Physics, V. I, p. 750, S. Hegarty et al. (eds.). Singapore: World Scientific 1992; B. De Lotto: Udine preprint 92/10/BL; Proc. XXVI Int. Conf. on High Energy Physics, Dallas, USA, 1992, J.R. Sanford (ed.). AIP Conference Proc. no. 272, p. 955
3. A. Białas, R. Peschanksi: Nucl. Phys. B273 (1986) 703
4. A. Białas, R. Peschanski: Nucl. Phys. B308 (1988) 857
5. E.A. De Wolf, I.M. Dremin, W. Kittel: Nijmegen preprint HEN-362 (1993); Brussels preprint IIHE-ULB-VUB-93-01, to be publ. in Phys. Rep. C
6. K. Fiałkowski: Phys. Lett. B272 (1991) 139; idem: in: Proc. Ringberg Workshop on Multiparticle Production, p. 238, R.C. Hwa, W. Ochs, N. Schmitz (eds.). Singapore: World Scientific 1992
7. E.L. Berger, R. Singer, G.H. Thomas, T. Kafka: Phys. Rev. D15 (1977) 206
8. G.H. Thomas: Phys. Rev. D15 (1977) 2636
9. M. Adamus et al., NA22 Coll.: Z. Phys. C32 (1986) 475
10. M. Adamus et al., NA22 Coll.: Z. Phys. C39 (1988) 311
11. A.H. Mueller: Phys. Rev. D4 (1971) 150
12. P. Lipa, P. Carruthers, H.C. Eggers, B. Buschbeck: Arizona preprint AZPHTH/91-53
13. P. Grassberger: Nucl. Phys. B120 (1977) 231
14. I.V. Ajinenko et al., NA22 Coll.: Z. Phys. C58 (1993) 357
15. I.V. Ajinenko et al., NA22 Coll.: Phys. Lett. B261 (1991) 165
16. B. Buschbeck, UA1 Coll.: Festschrift L. Van Hove, p. 211, A. Giovannini, W. Kittel. Singapore: World Scientific 1990
17. B. Andersson, G. Gustafson, B. Nilson-Almqvist: Nucl. Phys. B281 (1987) 289
18. A. Capella: in Proc. Europ. Study Conf. on Protons and Soft Hadronic Int., Erice, p. 199, R.T. Van de Walle (ed.). Singapore: World Scientific 1982; E.A. De Wolf: in Proc. XV Int. Symp. on Multiparticle Dynamics, Lund, Sweden 1984, p. 1. G. Gustafson, C. Peterson. Singapore: World Scientific 1984
19. T. Sjöstrand: Comput Phys. Commun. 39 (1986) 347
20. M. Bengtsson, T. Sjöstrand: Comput. Phys. Commun. 43 (1987) 367
21. M. Bengtsson, T. Sjöstrand: Nucl. Phys. B289 (1987) 810
22. G. Marchesini, B. Webber: Nucl. Phys. B310 (1988) 461
23. G. Marchesini, B. Webber: Cavendish-HEP-88/7 (1988)
24. I.V. Ajinenko et al., NA22 Coll.: Z. Phys. C51 (1991) 167
25. M.R. Atayan et al., NA22 Coll.: Z. Phys. C54 (1992) 247
26. P.D. Acton et al., OPAL Coll.: Phys. Lett. B305 (1993) 407
27. N.M. Agababyan et al., NA22: Z. Phys. C46 (1990) 387
28. C.T. Jones et al., WA21 Coll.: Z. Phys. C51 (1991) 11
29. W.D. Walker et al.: Phys. Lett. B255 (1991) 155
30. H. Albrecht et al., ARGUS Coll.: DESY preprint 93-083 (1993)
31. D. Buskelic et al., ALEPH Coll.: Phys. Lett. B292 (1992) 210
32. G. Gustafson, C. Sjögren: Phys. Lett. B248 (1990) 430
33. M. Gyulassy, S.K. Kauffmann, L.W. Wilson: Phys. Rev. C20 (1979) 2267
34. T. Sjöstrand: Comput. Phys. Commun. 27 (1982) 243
35. T. Sjöstrand, M. Bengtsson: Comput. Phys. Commun. 43 (1987) 367
36. W. Ochs: Phys. Lett. B247 (1990) 101; Z. Phys. C50 (1991) 339
37. A. Białas, M. Gazdzicki: Phys. Lett. B252 (1990) 483
38. N. Agababyan et al., NA22 Coll.: Z. Phys. C59 (1993) 405
39. F. Mandl, B. Buschbeck, DELPHI/UA1 Coll.: Proc. XXII Int. Symp. on Multiparticle Dynamics, Santiago de Compostela, Spain, 1992, p. 561. A. Pajares (ed.). Singapore: World Scientific
40. H.C. Eggers: PhD. Thesis, Univ. of Arizona, 1991
41. E.A. De Wolf: in: Proc. XXII Int. Symp. on Multiparticle Dynamics, Santiago de Compostela, Spain, 1992, p. 263, A. Pajares (ed.). Singapore: World Scientific
42. G. Gustafson: talk at Cracow Workshop on Soft Physics and Fluctuations, Cracow 1993, to be published; B. Andersson, G. Gustafson: private communication